Report of Investigation 2019-6

REGIONAL TSUNAMI HAZARD ASSESSMENT FOR SELECTED COMMUNITIES ON KODIAK ISLAND, ALASKA

E.N. Suleimani, J.B. Salisbury, D.J. Nicolsky, and R.D. Koehler

Kodiak Harbor. Photo: Barrett Salisbury.

Published by
STATE OF ALASKA
DEPARTMENT OF NATURAL RESOURCES
DIVISION OF GEOLOGICAL & GEOPHYSICAL SURVEYS

REGIONAL TSUNAMI HAZARD ASSESSMENT FOR SELECTED COMMUNITIES ON KODIAK ISLAND, ALASKA

E.N. Suleimani, J.B. Salisbury, D.J. Nicolsky, and R.D. Koehler

Report of Investigation 2019-6

State of Alaska
Department of Natural Resources
Division of Geological & Geophysical Surveys

STATE OF ALASKA
Michael J. Dunleavy, Governor

DEPARTMENT OF NATURAL RESOURCES
Corri A. Feige, Commissioner

DIVISION OF GEOLOGICAL & GEOPHYSICAL SURVEYS
Steve Masterman, State Geologist and Director

Publications produced by the Division of Geological & Geophysical Surveys (DGGS) are available for free download from the DGGS website (dggs.alaska.gov). Publications on hard-copy or digital media can be examined or purchased in the Fairbanks office:

Alaska Division of Geological & Geophysical Surveys
3354 College Rd., Fairbanks, Alaska 99709-3707
Phone: (907) 451-5010 Fax (907) 451-5050
dggspubs@alaska.gov | dggs.alaska.gov

DGGS publications are also available at:
Alaska State Library,
Historical Collections & Talking Book Center
395 Whittier Street
Juneau, Alaska 99811

Alaska Resource Library and Information Services (ARLIS)
3150 C Street, Suite 100
Anchorage, Alaska 99503

Suggested citation:
Suleimani, E.N., Salisbury, J.B., Nicolsky, D.J., and Koehler, R.D., 2019, Regional tsunami hazard assessment for selected communities on Kodiak Island, Alaska: Alaska Division of Geological & Geophysical Surveys Report of Investigation 2019-6, 31 p., 7 sheets. doi.org/10.14509/30195

Contents

Figures

Tables

Map Sheets

REGIONAL TSUNAMI HAZARD ASSESSMENT FOR SELECTED COMMUNITIES ON KODIAK ISLAND, ALASKA

E.N. Suleimani[1], J.B. Salisbury[2], D.J. Nicolsky[1], and R.D. Koehler[3]

Abstract

We assess potential tsunami hazard for the following seven coastal communities on Kodiak Island, Alaska: Akhiok, Chiniak, Karluk, Larsen Bay, Old Harbor, Ouzinkie, and Port Lions. The primary tsunami hazard for these communities is considered to be near-field, with a major threat originating from tsunamigenic earthquakes along the Alaska–Aleutian megathrust. We numerically model tsunamis generated by nine different megathrust earthquakes, analyze tsunami wave dynamics, and develop tsunami hazard maps for the seven communities. The hypothetical tsunami scenarios examined simulate M_W 9.0 megathrust earthquakes with a slip distribution in the 5–54 km (3–34 mi) depth range along the Alaska–Aleutian megathrust. The maximum runup heights are 14 m (46 ft) in Akhiok, 31 m (102 ft) in Chiniak, 11 m (36 ft) in Karluk, 18 m (59 ft) in Larsen Bay, 27 m (89 ft) in Old Harbor, 26 m (85 ft) in Ouzinkie, and 34 m (112 ft) in Port Lions. Results presented here are intended to provide guidance to local emergency management agencies in initial tsunami inundation assessment, evacuation planning, and public education for mitigation of future tsunami hazards.

INTRODUCTION

Tsunami hazards along Alaska's Pacific coastline are high. Virtually all of Alaska's southern and southeastern coasts are defined by major offshore fault systems. Unlike tsunamis that are caused by distant earthquakes on the other side of the Pacific, Alaska's greatest tsunami hazards originate just offshore and can inundate coastlines within an hour of a causative earthquake. This reduces the time available to respond and evacuate, and can produce drastically higher wave heights than far-traveled tsunamis. Because many Alaska communities hug the shoreline (due to some combination of steep mountains, dense forests, and/or reliance on the open water for transportation) many Alaska communities are within the tsunami inundation zone and are at risk of rapid flooding. In addition to earthquake-generated (i.e., tectonic) tsunamis, mass movements of sediments down slopes (either on land or in the ocean) can also generate tsunamis. While rapid tsunami flooding is the immediate concern after a large coastal earthquake, dangerous near-shore ocean currents and permanent changes to the local coastline are additional concerns.

The local, tectonic tsunami danger to communities in south-central Alaska comes primarily from the Alaska-Aleutian subduction zone (fig. 1). This subduction zone marks the boundary between the Pacific plate to the south and the North American plate to the north. Relative to the North American plate, the Pacific Plate is moving northwest at approximately 5–8 cm (2–3 inches) per year, colliding with the North American plate and diving beneath it in a process known as subduction. The latest sequence of large megathrust earthquakes began in 1938 with a M_W 8.3 earthquake west of Kodiak Island (Estabrook and others, 1994). Four subsequent events, the 1946 M_W 8.6 Aleutian (Lopez and Okal, 2006), 1957 M_W 8.6 Andreanof Islands (Johnson and others, 1994), 1964 M_W 9.2 Great Alaska Earthquake (Kanamori, 1970), and 1965 M_W 8.7 Rat Island (Wu and Kanamori, 1973) earthquakes,

[1]Alaska Earthquake Center, Geophysical Institute, University of Alaska, P.O. Box 757320, Fairbanks, Alaska 99775-7320; ensuleimani@alaska.edu
[2]Alaska Division of Geological & Geophysical Surveys, 3354 College Rd., Fairbanks, Alaska 99709-3707
[3]Nevada Bureau of Mines and Geology, Mackay School of Earth Science and Engineering, University of Nevada, Reno, 1664 North Virginia Street, MS 178, Reno, NV 89557

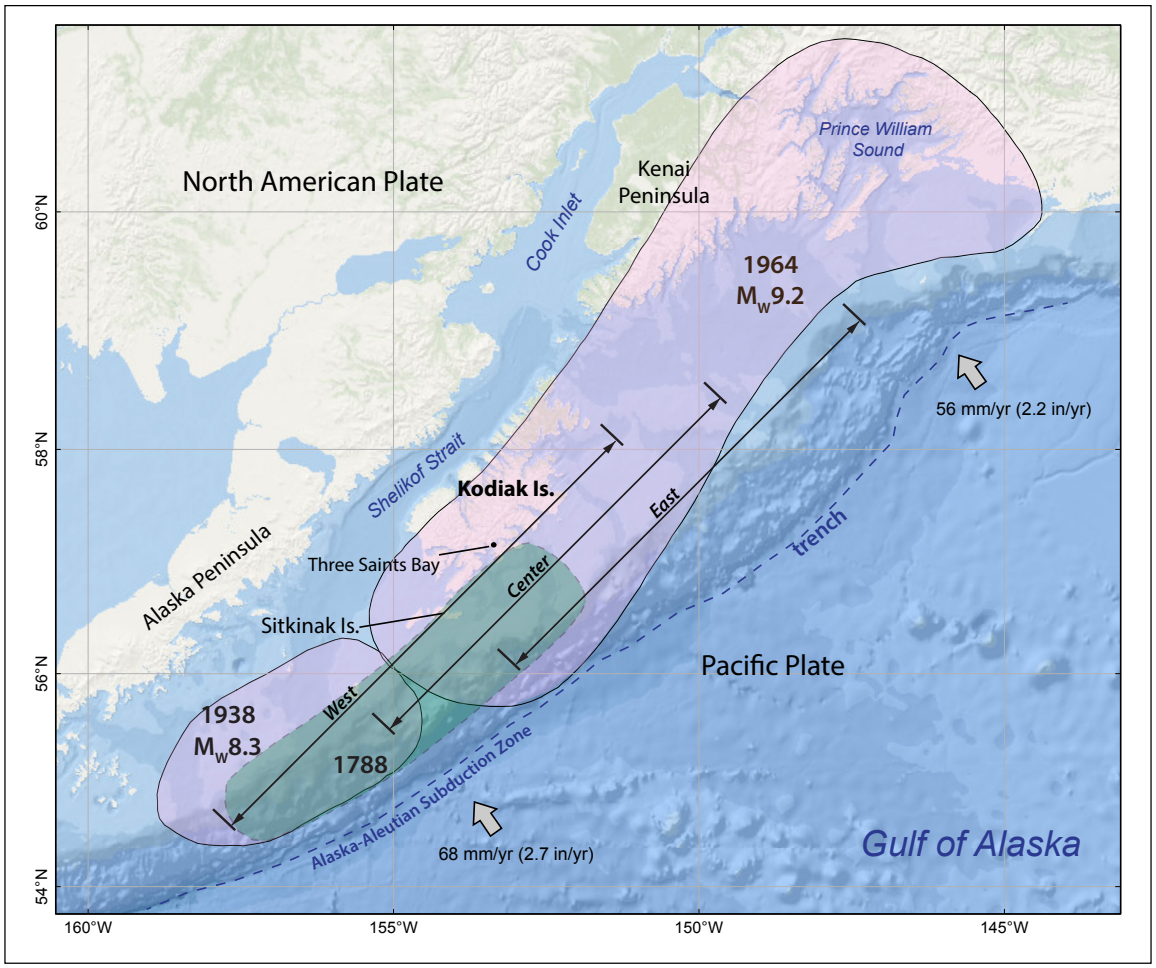

Figure 1. Map of south-central Alaska. The rupture areas of the 1938 and 1964 earthquakes are shown by pink-shaded polygons. Green polygon indicates the approximate rupture area of the 1788 earthquake. Black arrows indicate along-strike extents of the three regions on which the characteristic tsunami scenarios are based.

ruptured almost the entire length of the megathrust. Tsunamis generated by these great earthquakes reached Alaska coastal communities within minutes and resulted in widespread damage and loss of life (National Centers for Environmental Information [NCEI; formerly known as National Geophysical Data Center] Global Historical Tsunami Database, doi.org/10.7289/V5PN93H7).

The specifics of tsunami hazards are particular to each community and vary considerably over large regions. The shape of the coastline, local bathymetry, and topography all affect tsunami impacts. More importantly, however, is the earthquake source (the location, size, and style) being considered and the community's location relative to that earthquake.

The impacts of future earthquakes and tsunamis can be reduced if citizens, emergency managers, and city planners take steps to mitigate the hazards. This report is intended to support hazard mitigation efforts by providing approximate tsunami hazard estimates for the Kodiak communities of Akhiok, Chiniak, Karluk, Larsen Bay, Old Harbor, Ouzinkie, and Port Lions. The scenario earthquakes, numerical tsunami models, and resulting maps are developed on a regional level and lack the precision of studies that are fully tailored to individual communities (e.g., Nicolsky and others, 2013; Nicolsky and others, 2014; Suleimani and others, 2013, 2015). The current study does not include sensitivity tests and is based on multiple scenario earthquakes. Even so, the results provide a good first approximation

of tsunami hazard. The maps, documentation, and available digital data provide a foundation for public education, support the development of evacuation procedures, and provide insights intended to improve community resilience.

PROJECT BACKGROUND: REGIONAL AND HISTORICAL CONTEXT

Community Profiles

The following information is paraphrased from the Alaska Community Database Online provided by the Alaska Department of Commerce, Community, and Economic Development, Division of Community and Regional Affairs (DCCED/DCRA, 2013).

Figure 2 shows locations of communities on Kodiak Island.

Akhiok (56°56'40"N, 154°10'13"W), population 81, is Kodiak's southernmost village and is located on the northwestern coast of Alitak Bay. It is 129 km (80 mi) southwest of Kodiak and 547 km (340 mi) southwest of Anchorage. Akhiok is an Alutiiq village that depends on fishing and subsistence activities.

Chiniak (57°36'38"N, 152°11'59"W), population 48, is on the easternmost point of Kodiak Island, 72 km (45 mi) southeast of Kodiak. Captain Cook originally named this location Point Greville in 1778. During the mid-1950s, an Air Force radar tracking station was constructed in Chiniak. The community can be reached by road from Kodiak, and also by floatplane, ferry, and boat.

Karluk (57°34'41"N, 154°21'45"W), population 43, is on the west coast of Kodiak Island on the banks of Karluk Lagoon, 142 km (88 mi) southwest of Kodiak and 484 km (301 mi) southwest of Anchorage. The mouth of the Karluk River is thought to have been populated by Alaska Natives for more than 7,000 years. Russian hunters established a trading post here in 1786. By 1900 Karluk was known for having the largest cannery and the greatest salmon stream in the world. Karluk is an Alutiiq village with a fishing and subsistence lifestyle.

Larsen Bay (57°32'12"N, 153°59'29"W), population 71, is an Alutiiq village named after the bay on which it sits on the northwest coast of Kodiak Island. It is 97 km (60 mi) southwest of Kodiak and 455 km (283 mi) southwest of Anchorage. The area is thought to have been inhabited for at least 2,000 years. The bay was named for Peter Larsen, an Unga Island furrier, hunter, and guide. The economy of Larsen Bay is primarily based on fishing, and a large majority of the population depends on subsistence activities. Salmon, halibut, seal, sea lion, clams, crab, and deer are harvested. Six lodges host visitors and provide a tourist guide service.

Old Harbor (56°56'40"N, 154°10'13"W), population 213, is an Alutiiq community on the southeast coast of Kodiak Island, 113 km (70 mi) southwest of the Kodiak and 518 km (322 mi) southwest of Anchorage. The area around Old Harbor is thought to have been inhabited for nearly 2,000 years. The area was visited by the Russian Grigori Shelikov and his *Three Saints* flagship in 1784. Three Saints Bay became the first Russian colony in Alaska. In 1788, a tsunami destroyed the settlement. A settlement was re-established at Three Saints Harbor in 1884. The town was recorded as "Staruigavan," meaning "old harbor" in Russian. The Old Harbor post office was opened in 1931. In 1964, the Great Alaska Earthquake and resulting tsunami destroyed the community; only two homes and the church remained standing. The community was rebuilt in the same location. Old Harbor practices its traditional Alutiiq culture and subsistence lifestyle. Fishing provides income to the community.

Ouzinkie (57°55'24"N, 152°30'07"W), population 171, is an Alutiiq village on

the west coast of Spruce Island, adjacent to Kodiak Island. It is 16 km (10 mi) northwest of Kodiak and 398 km (247 mi) southwest of Anchorage. Ouzinkie started as a retirement community for the Russian American Company. In 1889, the Royal Packing Company constructed a cannery at Ouzinkie. In 1890 a Russian Orthodox church was built, and in 1927 a post office was established. In 1964, the Great Alaska Earthquake and resulting tsunami destroyed the Ouzinkie Packing Company cannery. The city government was incorporated in 1967. Commercial fishing and subsistence activities support the community.

Port Lions (57°52'5"N, 152°52'48"W), population 176, is an Alaska Native village in Settler Cove on the north coast of Kodiak Island, 399 km (248 mi) southwest of Anchorage. The town was founded in 1964 by the displaced inhabitants of Afognak, which was destroyed by a tsunami after the Great Alaska Earthquake. The community was named in honor of the local Lions Club for their support in rebuilding and relocating the village. The city government was incorporated in 1966. The majority of the population is Alutiiq. Most residents lead a fishing and subsistence lifestyle.

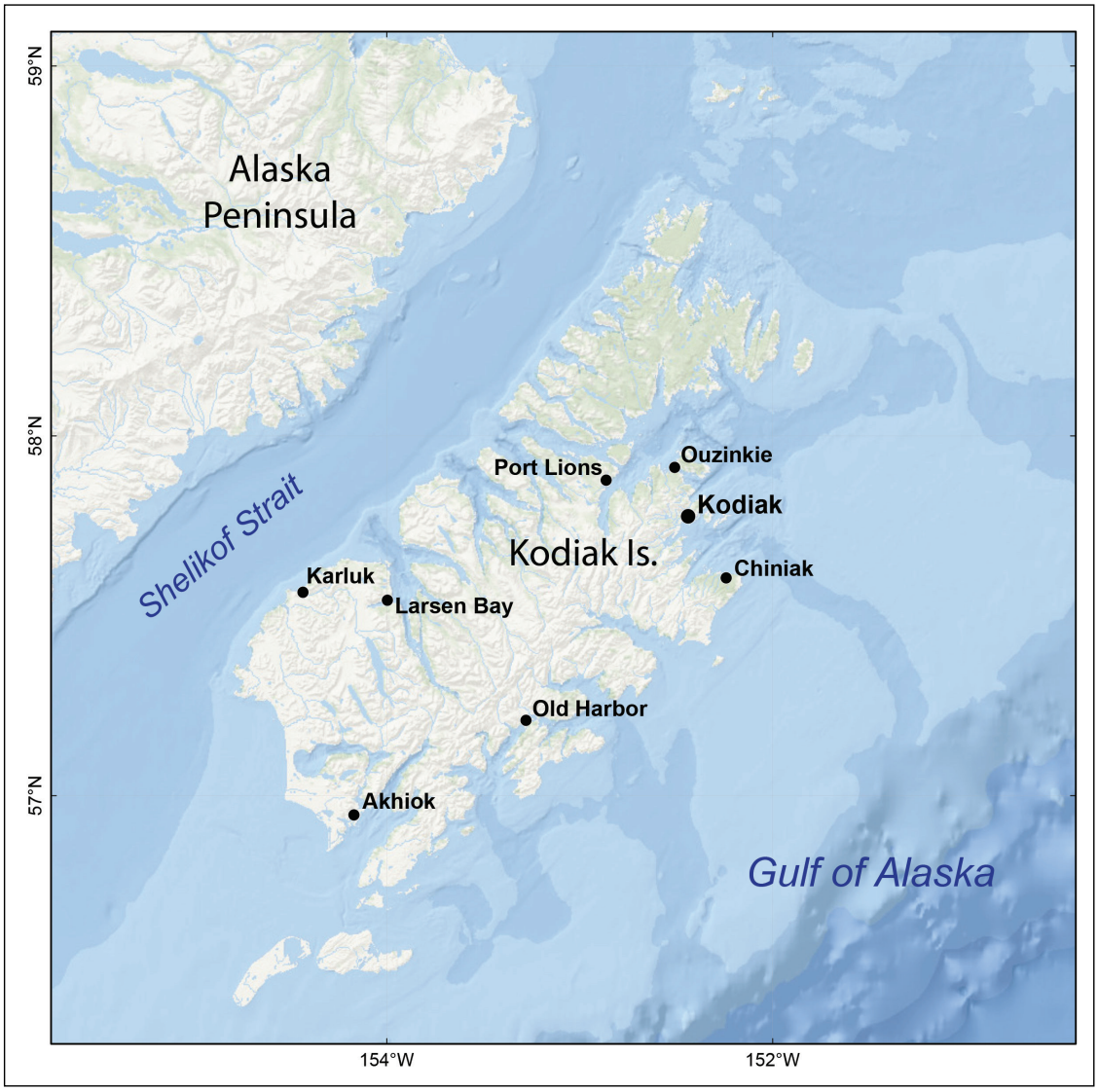

Figure 2. Map of Kodiak Island, showing locations of coastal communities.

Seismic and Tsunami History

Kodiak Island is situated near the eastern end of the Alaska–Aleutian subduction zone, the boundary along which the Pacific and North American plates converge (fig. 1). The rate of plate convergence near the island is approximately 60 mm (2.4 in) per year (DeMets and others, 1990). The eastern end of the megathrust has produced significant tsunamigenic earthquakes in the past. On March 27, 1964, south-central Alaska was struck by the largest earthquake ever recorded in North America. This M_W 9.2 megathrust event (fig. 1), known as the Great Alaska Earthquake, generated a destructive tsunami that caused fatalities and great damage in Alaska, Hawaii, and the west coast of the contiguous United States and Canada. The earthquake ruptured an 800-km-long (~500-mi-long) section of the Aleutian megathrust, producing vertical displacements over an area of about 285,000 km^2 (110,039 mi^2) in south-central Alaska (Plafker, 1969). The area of coseismic subsidence included Kodiak Island, Kenai Peninsula, Cook Inlet, and part of northern Prince William Sound (fig. 1). The major zone of uplift was seaward of the subsidence zone, in Prince William Sound and the Gulf of Alaska (Plafker, 1969). Of the 131 fatalities associated with this earthquake, 122 were caused by tsunamis (Lander, 1996). A number of communities on Kodiak Island suffered greatly from tsunami waves. The penultimate tsunami event in the area of Kodiak Island was recorded on July 21, 1788, when a strong earthquake near Sitkinak Island caused a 3–10 m (10–33 ft) tsunami that forced relocation of the first Russian settlement at Three Saints Bay (now Old Harbor) on southwestern Kodiak Island (Lander, 1996) (fig. 1). Briggs and others (2014) found stratigraphic evidence of land level change and sand deposits that can be traced 1.5 km (1 mi) inland on Sitkinak Island (fig. 1). Cesium-lead (^{137}Cs and ^{210}Pb) age estimates for the sand suggest that the 1788 megathrust rupture generated this devastating tsunami.

According to Lander (1996) and the Global Historical Tsunami Database of the National Centers for Environmental Information (NCEI), National Oceanic & Atmospheric Administration (NOAA) (doi.org/10.7289/V5PN93H7), all Kodiak communities were affected by the 1964 Great Alaska Earthquake and tsunami. Table 1 summarizes all historically recorded tsunami events that produced wave heights greater than 15 cm (0.5 ft) at the communities considered in this report.

METHODOLOGY AND DATA

Methodology

The regional tsunami hazard maps presented here are the product of collaborative efforts between state and federal agencies to assist coastal communities in Alaska with tsunami hazard assessment. In recent years, similar tsunami hazard studies have been published for other communities (Nicolsky and others, 2011a; Nicolsky and others, 2013; Nicolsky and others, 2014; Suleimani and others, 2010; Suleimani and others, 2013; 2015). Because the currently available digital elevation models (DEMs) for these Kodiak Island communities are of insufficient quality for high-resolution modeling, we follow the National Tsunami Hazard Mitigation Program (NTHMP, 2010) guidelines (nws.weather.gov/nthmp/publications.html) for determining tsunami hazard zones for areas that have either low risk due to small population size and minimal infrastructure vulnerability, or do not have access to high-resolution tsunami inundation maps. The tsunami hazard maps for the communities evaluated in this study are developed using the methodology described in detail in Suleimani and others (2018). In short, for nine scenario earthquakes, we modeled water dynamics from source to community and computed maximum tsunami wave heights using the highest resolution grids available (see table 2). Each model run covers 6 hours of post-earthquake tsunami propagation to account for all waves in the wave train, as well as secondary (reflected) wave interactions. At every location throughout the high-resolution grids, the maximum tsunami height from any of the nine earthquakes is saved, and we use these maximum values to extrapolate wave runup heights on land in a new, "composite" map of maximum wave heights that can be expected from the earthquake scenarios.

Table 1. Tsunami effects at selected Kodiak communities. Data from the National Centers for Environmental Information (NCEI; formerly known as National Geophysical Data Center [NGDC]) Global Historical Tsunami Database (doi.org/10.7289/V5PN93H7) and comments from Lander (1996).

Date	Magnitude (MW)	Origin	Maximum water height, m (ft)	Comments
Akhiok				
03/28/1964	9.2	Gulf of Alaska	15.0 (49.2)	Homes and boats destroyed.
Chiniak				
03/28/1964	9.2	Gulf of Alaska	9.1 (30.0)	Cape Chiniak observed the first tsunami wave about 30 minutes after the earthquake.
Larsen Bay				
03/28/1964	9.2	Gulf of Alaska	1.22 (4.0)	Warehouse flooded, sheds destroyed, and cattle drowned.
Old Harbor				
07/21/1788	?	Alaska Peninsula	3–10 (10-33)	Ship cast on shore; several huts destroyed.
03/28/1964	9.2	Gulf of Alaska	7.3 (24.0)	Village nearly destroyed, $150,000 damage (1964 dollars), one death.
02/27/2010	8.8	Maule, Chile	0.51 (1.7)	
03/01/2011	9.0	Honshu, Japan	0.38 (1.2)	
Ouzinkie				
03/28/1964	9.2	Gulf of Alaska	9.14 (30.0)	The community suffered extensive damage, about $500,000. Cannery, post office, and company store were destroyed. Waterfront was extensively damaged and commercial fishing gear was destroyed.

Computational Grids and Data Sources

To develop a regional tsunami hazard map we use a series of nested computational grids. A nested grid allows for higher resolution in areas where it is needed without expending computer resources in areas where it is not. The bathymetric and topographic relief in each nested grid is based on DEMs developed at the NCEI. The extent of each grid used in this mapping project is shown in figure 3 and listed in table 2. The coarsest grid, level 0, with 2-arc-minute (approximately 2 km [1.2 mi]) resolution, spans the central and northern Pacific Ocean. The bathymetric data for the 2-arc-minute-resolution grid is extracted from the ETOPO2 dataset (NGDC, 2006, doi.org/10.7289/V5J1012Q). We use two intermediate grids between the coarsest- and highest-resolution grids (table 2). The first intermediate grid of 24 arc-second resolution (level 1) was developed to accommodate the current tsunami mapping project for Kodiak Island as well as other tsunami mapping efforts for communities located on the Kenai Peninsula and around Prince William Sound. The data sources and methodology used to develop the 24-arc-second DEMs

Table 2. Nested grids used to compute propagation of tsunami waves generated in the Pacific Ocean to the seven Kodiak Island communities. The fine-resolution grid is used to compute the inundation. Note that the grid resolution in meters is not uniform and is used to illustrate grid fineness in the Kodiak Island region. The first dimension is the longitudinal grid resolution; the second is the latitudinal resolution.

Grid name	Resolution		West–East boundaries	South–North boundaries
	Arc-seconds	Meters (near Kodiak)		
Level 0, Northern Pacific	120 × 120	≈ 2,015 × 3,700	120°00′ E–100°00′ W	10°00′ N–65°00′ N
Level 1, South-central Alaska	24 × 24	≈ 403 × 740	156°00′ W–145°00′ W	55°00′ N–62°00′ N
Level 2, Coarse resolution, Kodiak Island	8 × 8	≈ 135 × 247	155°38′36″ W–149°50′33″ W	56°01′45″ N–59°02′06″ N
Level 3, Fine resolution, Kodiak Island	8/3 × 8/3	≈ 45 × 82	155°01′02″ W–151°39′19″ W	56°18′59″ N–58°48′49″ N

are described in detail by Lim and others (2011). The 8- and 8/3-arc-second DEMs were developed by the NCEI in the scope of NTHMP by interpolating the datasets used to produce the southern Alaska 24-arc-second coastal relief model at the appropriate resolution. These datasets include soundings from hydrographic surveys and digitized nautical charts, tracklines, and multibeam swath sonar data with spatial resolution ranging from 10 to 1,000 meters. The Kodiak Island 1-arc-second DEM was also used in the interpolation process.

The fine-resolution grid for Kodiak covers the entire island. The size of the fine-resolution grid cells, which is about 45 × 82 m (148 × 269 ft), satisfies NOAA's minimum recommended requirements for estimation of the tsunami hazard zone (NTHMP, 2010); however, no DEM verification efforts were conducted to reduce uncertainties in the Kodiak high-resolution (level 3) grid. Therefore, in this report we do not perform high-resolution runup modeling, but provide an estimation of the tsunami hazard zone by extrapolating the maximum composite tsunami wave height on land according to the tsunami scenarios described below. We account for uncertainties inherent to this method by applying a safety factor of 1.3 (Suleimani and others, 2018) to the estimated hazard zone.

Tsunami Sources

In this project we use a deterministic approach to develop potential tsunami sources, which is distinctly different from the probabilistic tsunami hazard analyses used in projects with different objectives, such as land-use planning or insurance estimates (Geist and Parsons, 2006). Alaska tsunami hazard maps are produced on the basis of significant credible tsunami scenarios for a given segment of the coastline. Although we do not explicitly develop worst-case credible tsunami scenarios in this report as we have in some previous reports, we use the same underlying assumptions and results regarding the maximum considered earthquake scenarios for other locations along the Alaska-Aleutian subduction zone.

In this regional tsunami hazard assessment we consider three characteristic tsunamigenic earthquake scenarios (e.g., Suleimani and others, 2018). These potential megathrust ruptures have a uniform slip distribution along strike, but differ in the downdip slip distribution pattern such that the depth range at which the maximum slip occurs varies from the shallow region close to the trench to the deeper parts of the plate interface. Because the Kodiak communities considered in this report

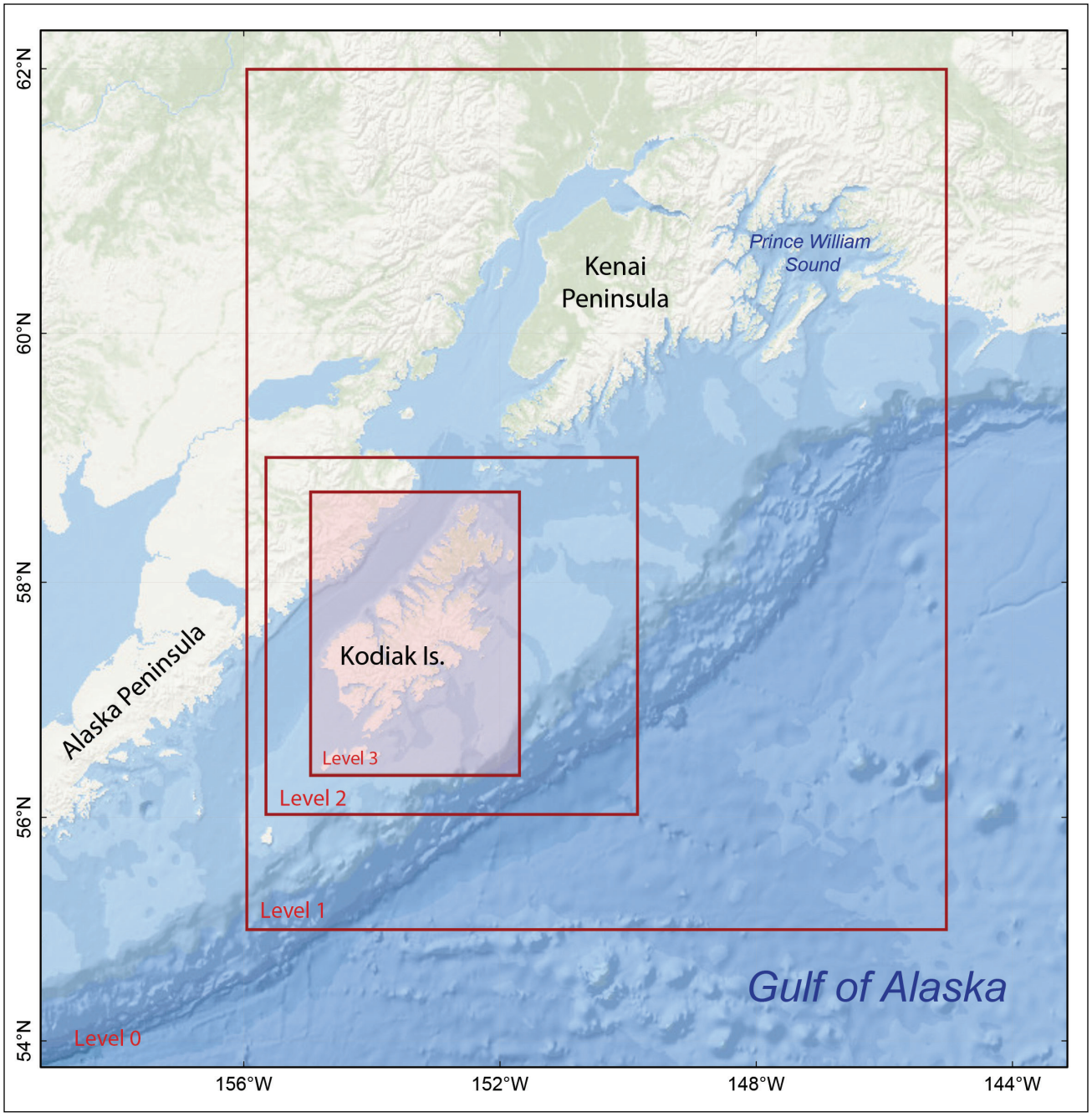

Figure 3. Nesting of the bathymetry/topography grids for numerical modeling of tsunami propagation and runup. The coarsest grid, level 0, covers the central and northern Pacific Ocean. The location of each embedded grid is marked by a red rectangle. Refer to table 2 for grid parameters.

are spread around the entire island, we place each characteristic scenario in three different, partially overlapping regions along the subduction interface in order to cover all possible tsunami effects for each community. Using scenario 1 as an example, we illustrate in figure 1 the three different along-strike segments: the west, center, and east iterations for this scenario. The same three iterations are used for scenarios 2 and 3, which gives us the nine tsunami sources that we use in this study to assess tsunami hazard for the selected Kodiak Island communities. All ruptures have the same extent, which is determined by the location of communities and constrained by the seismic moment. Refer

to Suleimani and others (2018) for a description of the scenario development and for the proposed slip distributions.

The three characteristic tsunami scenarios for Kodiak communities are outlined below. The vertical coseismic deformations for scenarios 1, 2, and 3 are shown in figures 4A, 4B, and 4C, respectively. The main rupture parameters are listed in table 3, and the amount of permanent subsidence for each community is given in table 4.

Scenario 1. M_W 9.0 earthquake: SAFRR-type event applied to the west, center, and east segments (fig. 1)

A hypothetical Tohoku-type M_W 9.0 earthquake rupturing the Alaska–Aleutian megathrust. During the 2011 Tohoku, Japan, earthquake a large amount of slip occurred in a shallow region between the subducting and overriding plates near the Japan trench (Fujii and others, 2011; Shao and others, 2011). The USGS Science Application for Risk Reduction (SAFRR) project, in collaboration with NOAA and State of California agencies, developed a plausible hypothetical tsunami scenario (Kirby and others, 2013) to describe the impacts of a tsunami generated by a similar earthquake in the Alaska Peninsula region (Ross and others, 2013). Here we assume that the slip distribution in the downdip direction is the same as that in the SAFRR source, where the greatest slip occurs close to the seafloor trench. The slip is distributed almost uniformly along strike except for the edges of the rupture, where it tapers. The maximum slip of 46 m (151 ft) is at a depth of 5–15 km (3–9 mi).

Scenario 2. M_W 9.0 earthquake: Maximum slip at 15–25 km (9–15 mi) depth applied to the west, center, and east segments (fig. 1)

A hypothetical M_W 9.0 earthquake rupturing the Alaska–Aleutian megathrust. The slip is distributed almost uniformly along strike except for the edges of the rupture, where it tapers. The maximum slip of 35 m (115 ft) is at a depth of 15–25 km (9–16 mi).

Scenario 3. M_W 9.0 earthquake: Maximum slip at 25–35 km (15–21 mi) depth applied to the west, center, and east rupture segments (fig. 1)

A hypothetical M_W 9.0 earthquake rupturing the Alaska–Aleutian megathrust. The slip is distributed almost uniformly along strike except for the edges of the rupture, where it tapers. The maximum slip of 35 m (115 ft) is at a depth of 25–35 km (16–22 mi).

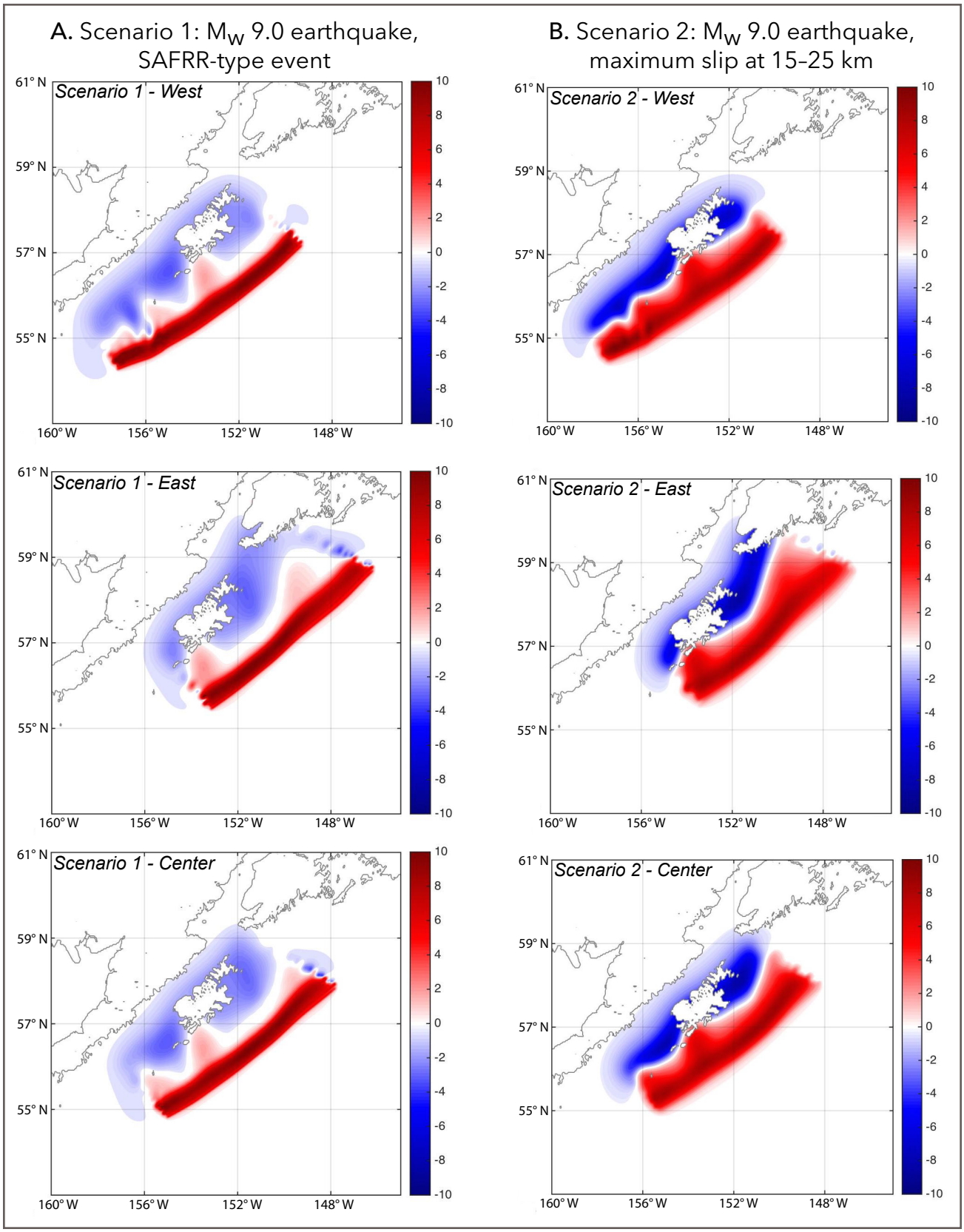

Figure 4. Vertical coseismic deformations corresponding to scenarios 1 and 2. Blue areas are associated with coseismic ground subsidence; areas of uplift are shown in red.

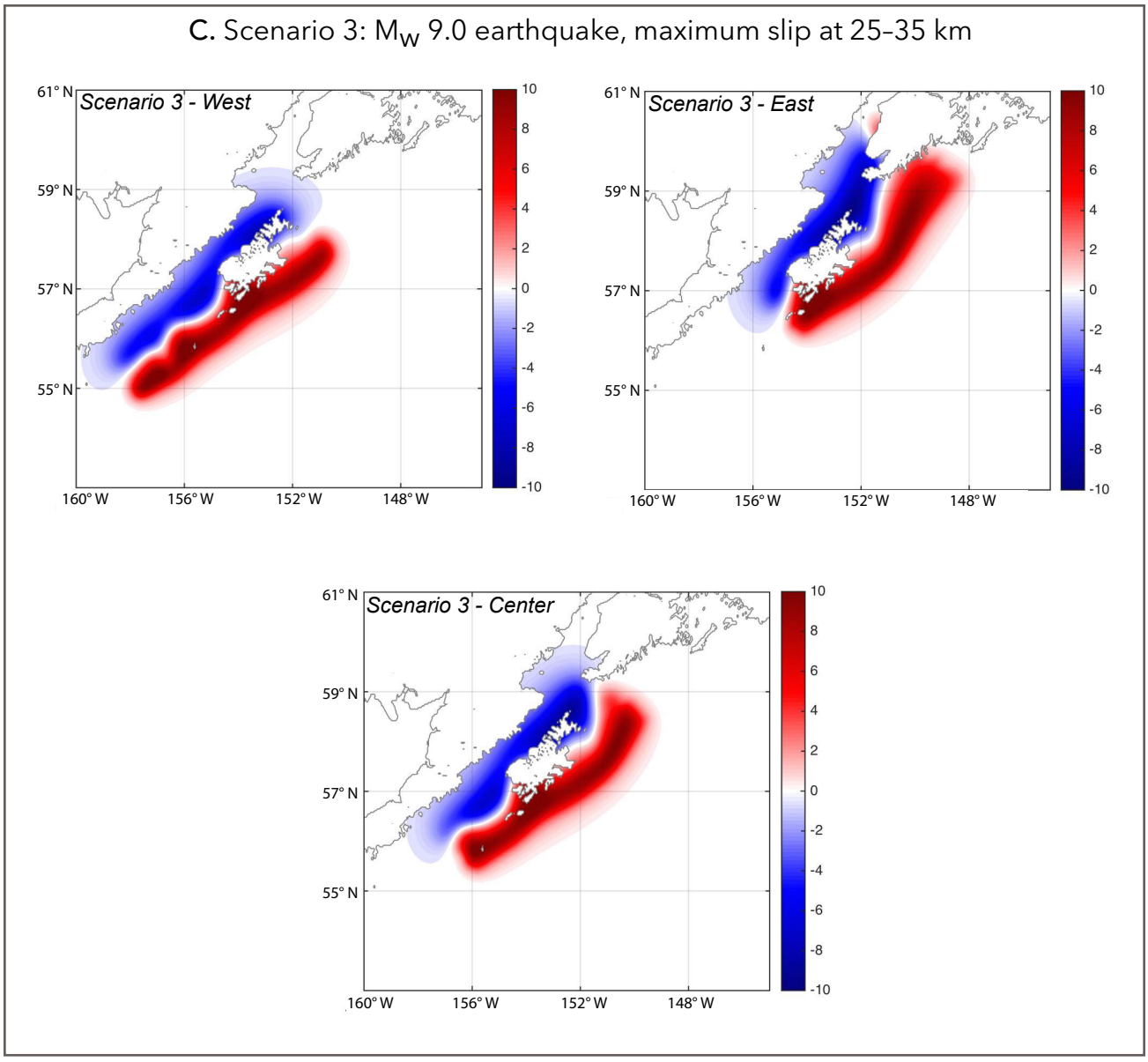

Figure 4, continued. Vertical coseismic deformations corresponding to scenario 3. Blue areas are associated with coseismic ground subsidence; areas of uplift are shown in red.

Numerical Model of Tsunami Propagation and Runup

The numerical model currently used by the Alaska Earthquake Center for tsunami inundation mapping is a nonlinear, flux-formulated, shallow-water model (Nicolsky and others, 2011b) that has been validated (NTHMP, 2012) through a set of analytical benchmarks and tested against laboratory and field data (Synolakis and others, 2007). The application of the model to tsunami inundation mapping of Alaska coastal communities, including its assumptions and limitations, is described in a number of previous tsunami reports (e.g., Suleimani and others, 2018). In this study, we conduct all model runs using bathymetric data that correspond to the Mean Higher High Water (MHHW) tide level in the Kodiak communities.

For each tsunami scenario, we first calculate the maximum tsunami wave heights in the highest-resolution grid over the course of the entire

Table 3. Significant credible tectonic tsunami sources for Kodiak communities.

Scenarios		Depth range, km (mi)	Maximum slip depth range, km (mi)	Maximum slip, m (ft)	Maximum regional subsidence, m (ft)	Maximum regional uplift, m (ft)
1	M_W 9.0 earthquake: SAFRR-type event, slip near the trench	8–54 (5–34)	11–14 (7–8.7)	55–65 (180–213)	-4.0 (-13.1)	10.3 (33.8)
2	M_W 9.0 earthquake: Maximum slip at 15–25 km (9.3–15.5 mi) depth	5–35 (3–21.7)	15–25 (9.3–15.5)	34–35 (112–115)	-8.6 (-28.2)	8.8 (28.9)
3	M_W 9.0 earthquake: Maximum slip at 25–35 km (15.5–21.7 mi) depth	14–45 (8.7–28)	25–35 (15.5–21.7)	34–35 (112–115)	-9.6 (-31.5)	11.8 (38.7)

Table 4. Summary of tsunami modeling results for the Kodiak Island communities. "Actual subsidence" is the permanent subsidence that the model shows for the community, which may be (significantly) less than the maximum expected subsidence across the entire region for that same earthquake scenario. Maximum assumed runup height is the maximum composed tsunami height multiplied by the safety factor of 1.3.

Community	Maximum composite tsunami height, m (ft)	Maximum estimated runup height, m (ft)	Actual subsidence in communities, m (ft)	Composite tsunami height	Tsunami hazard map	Calculated time series
Akhiok	10.8 (35.4)	14 (46)	-0.5 (-1.6)	Figure 6A	Map sheet 1	Figure 7A
Chiniak	23.8 (78.1)	31 (102)	-5.9 (-19.4)	Figure 6B	Map sheet 2	Figure 7B
Karluk	8.5 (27.9)	11 (36)	-3.6 (-11.8)	Figure 6C	Map sheet 3	Figure 7C
Larsen Bay	13.8 (45.3)	18 (59)	-5.1 (-16.7)	Figure 6D	Map sheet 4	Figure 7D
Old Harbor	20.8 (68.2)	27 (89)	-1.2 (-3.9)	Figure 6E	Map sheet 5	Figure 7E
Ouzinkie	20 (65.6)	26 (85)	-7 (-23)	Figure 6F	Map sheet 6	Figure 7F
Port Lions	26 (85.3)	34 (112)	-6.3 (-20.7)	Figure 6G	Map sheet 7	Figure 7G

model run in the following way: at each grid point, the tsunami wave height is computed at every time step during the tsunami propagation time, and the maximum value is kept. Then we compute the composite maximum wave height from all considered scenarios by again choosing the maximum value for each grid point among all scenarios, and plot the results.

MODELING RESULTS

We performed numerical calculations for three iterations (west, center, east) of each of the three earthquake scenarios for a total of nine unique tsunamigenic earthquake scenarios. Figures 5A–5C show the maximum tsunami heights for scenarios 1–3, respectively, in the Kodiak level 3 grid. All three sources in scenario

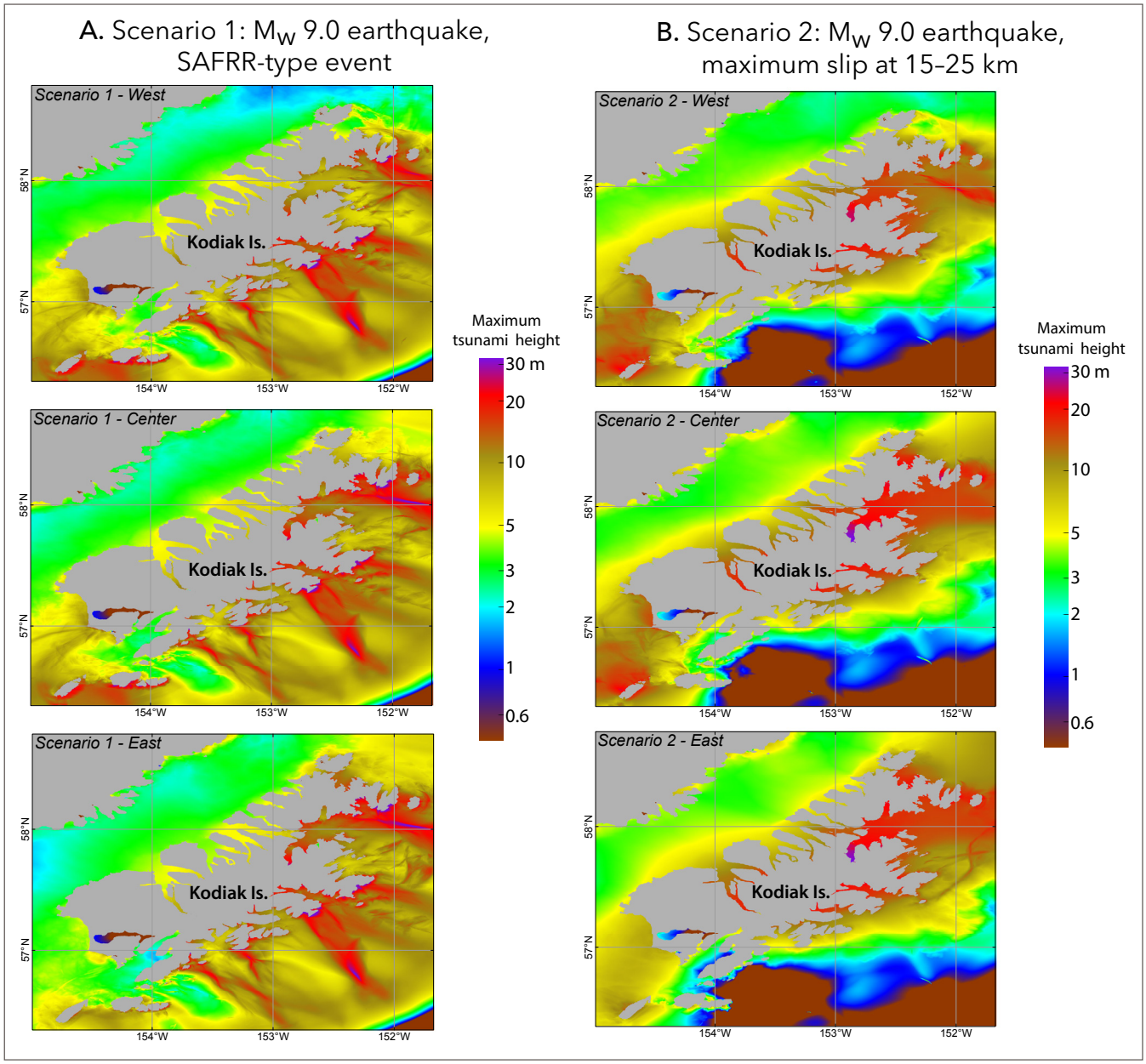

Figure 5. Maximum tsunami heights for scenarios 1 and 2 in the Kodiak level 3 grid.

1 produce the largest amplitudes along the southeastern coast of the island. The sources in scenario 3 generate much smaller waves along this coast, but result in large waves in the Shelikof Strait, along the northwestern coast of Kodiak Island.

Figure 6 shows maps of the maximum composite tsunami height for all nine scenarios, calculated in the vicinity of all seven communities. In these figures, the mismatch between the coastlines of the base imagery and the coastlines corresponding to the data set is due to the resolution of the level 3 Kodiak DEM. Table 4 summarizes all modeling results and provides the maximum value of the tsunami height for each community. This value, multiplied by a safety factor of 1.3, gives the maximum estimated runup height for each community. We project the value of the maximum estimated runup height on land by drawing an elevation contour on a community topographic map that corresponds to this height. This contour is the approximate boundary of the tsunami hazard zone, and should be used by emergency planners and public officials as a guide in tsunami mitigation activities.

Map sheets 1–7 are approximate tsunami hazard maps for the Kodiak communities. For all communities except for Chiniak, we used the DCRA elevation datasets and the 2014 GPS surveys to reference the DCRA elevation contours to the MHHW datum (Macpherson and others, 2014). For each community, we selected the closest contour to the estimated maximum composite wave height and extracted it as the tsunami hazard boundary. Where DRCA data are incomplete for a community, we infer contours based on available imagery or other, lower-resolution DEMs and use a different map symbol to represent these areas. No DCRA elevation data existed for Chiniak, therefore we extracted the elevation contour of 31 m (102 ft) from the 1/3-arc-second DEM of Chiniak. Refer to the metadata that accompanies this report for more details.

To help emergency managers understand the duration of tsunami hazard after a large megathrust earthquake, we supplement the hazard maps with the time series of the modeled water level at a nearshore location in each community (white triangles in figure 6). Time series plots are shown in figure 7, with zero time corresponding to the time when the earthquake occurs. To compare the height of arriving tsunamis for different scenarios—which result in different values of land subsidence—we use a vertical datum with a zero mark corresponding to the post-earthquake sea level. The time series

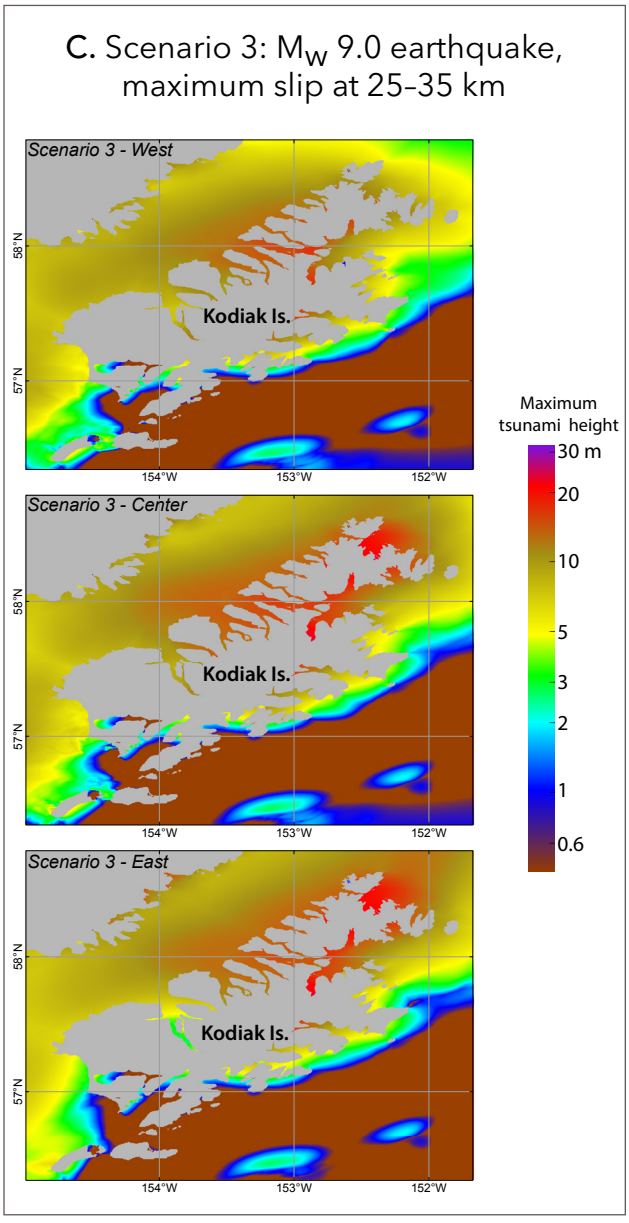

Figure 5, continued. Maximum tsunami height for scenario 3 in the Kodiak level 3 grid.

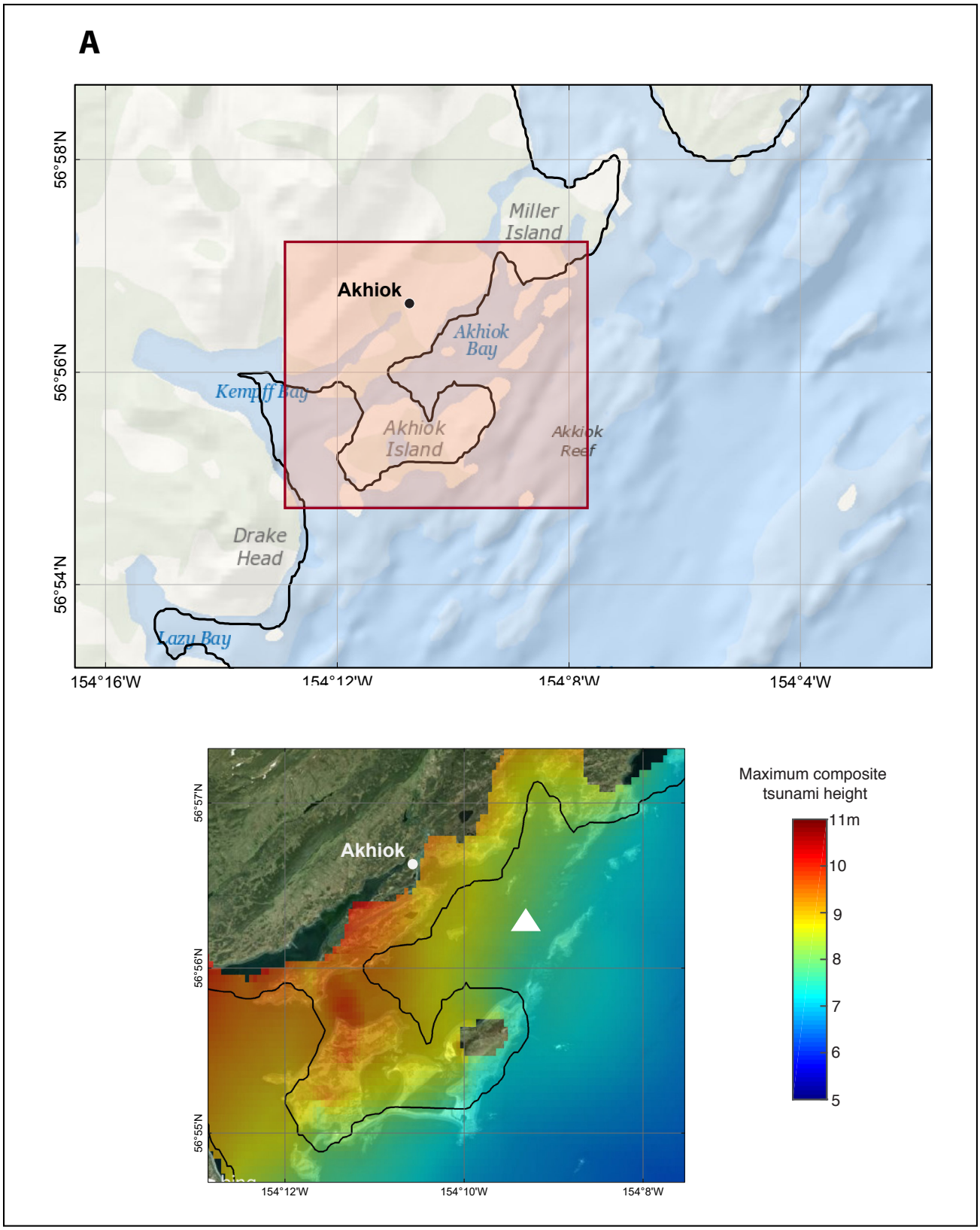

Figure 6A. Maximum composite tsunami height at Akhiok. The white triangle indicates the location of the time series point, and the black line is the MHHW shoreline. The pink shaded rectangle in the upper map indicates the area shown in the lower map. The mismatch between the coastlines of the base imagery and the MHHW coastlines is due to low resolution of the level 3 Kodiak DEM.

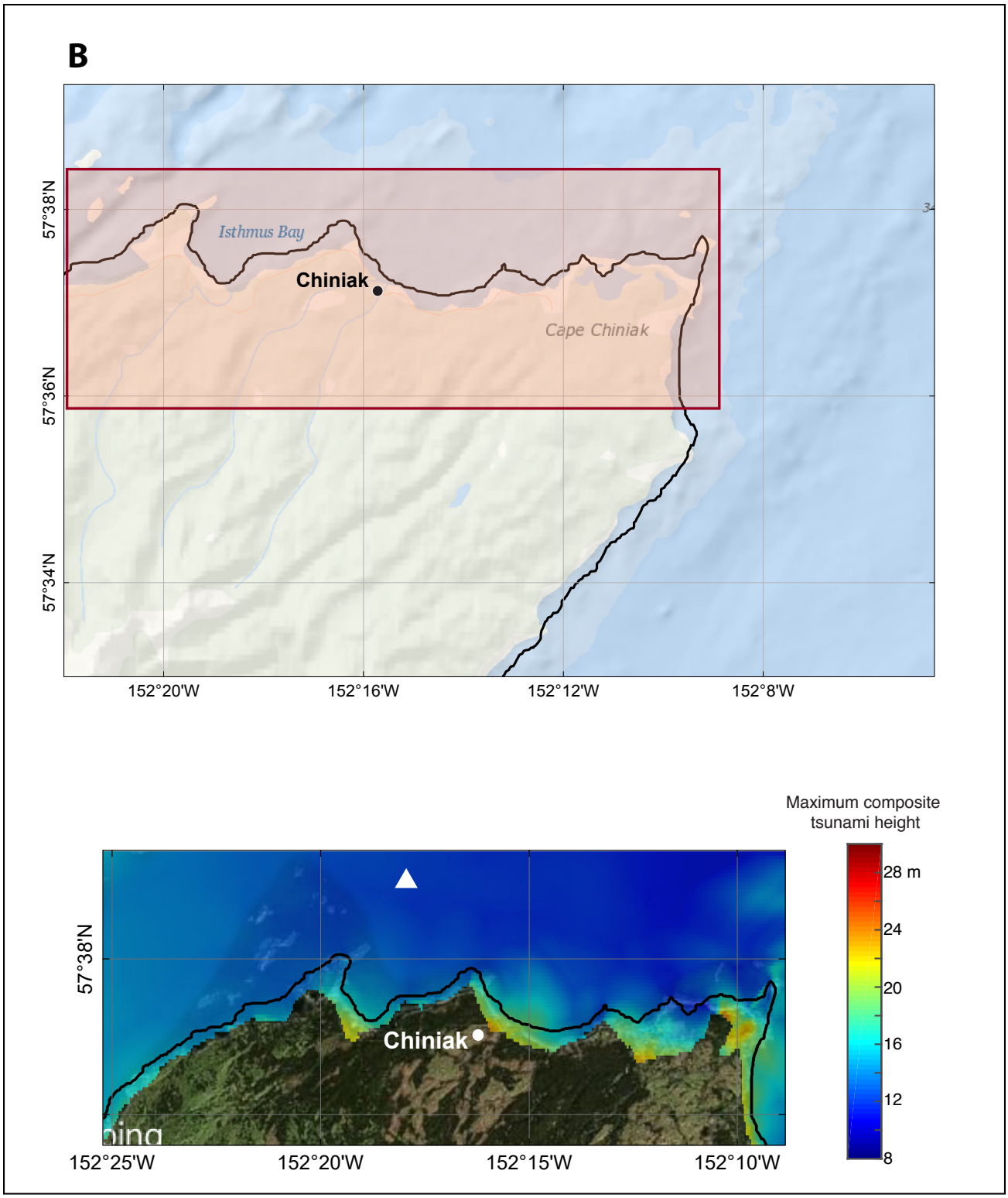

Figure 6B. Maximum composite tsunami height at Chiniak. The white triangle indicates the location of the time series point, and the black line is the MHHW shoreline. The pink shaded rectangle in the upper map indicates the area shown in the lower map. The mismatch between the coastlines of the base imagery and the MHHW coastlines is due to low resolution of the level 3 Kodiak DEM.

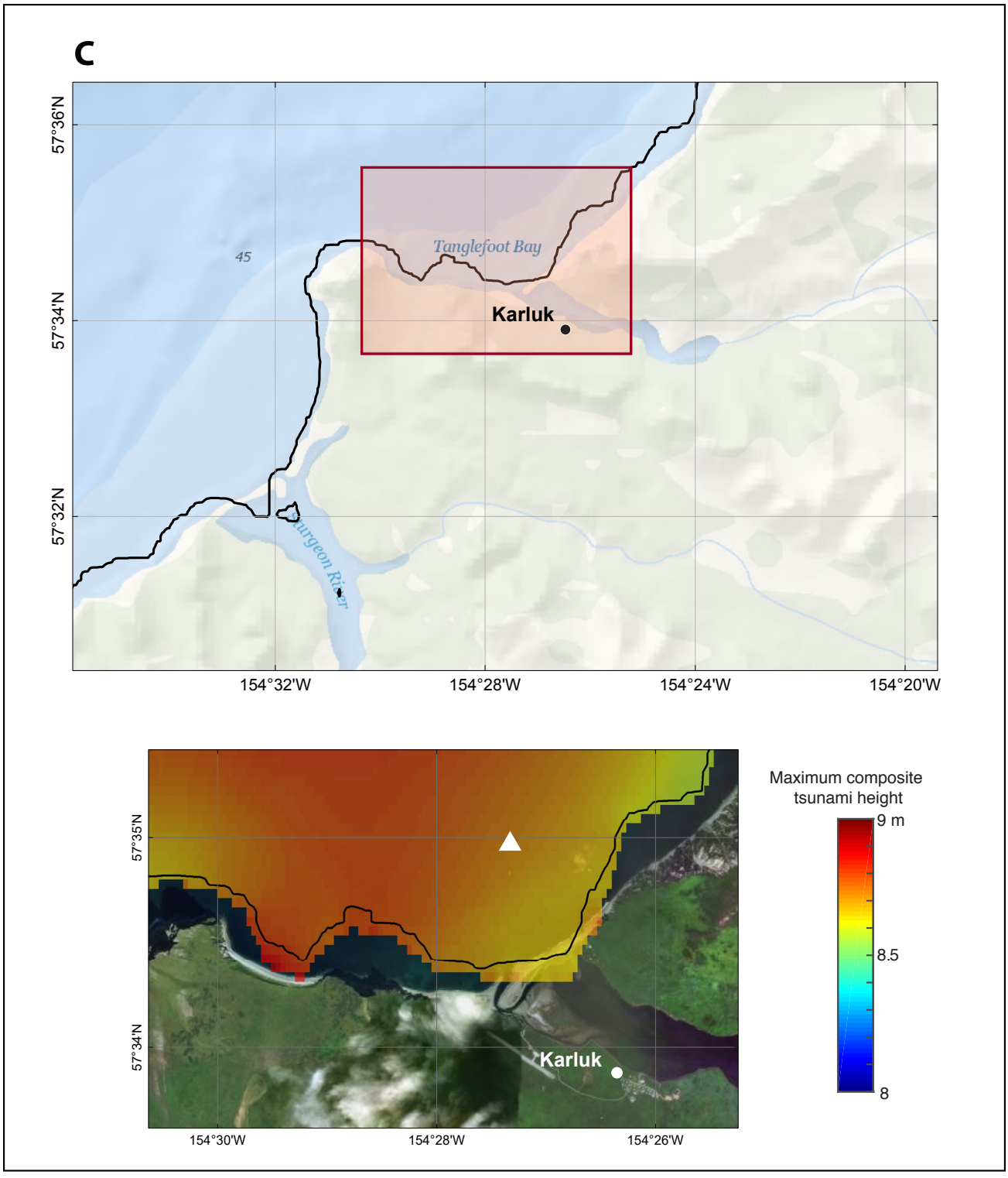

Figure 6C. Maximum composite tsunami height at Karluk. The white triangle indicates the location of the time series point, and the black line is the MHHW shoreline. The pink shaded rectangle in the upper map indicates the area shown in the lower map. The mismatch between the coastlines of the base imagery and the MHHW coastlines is due to low resolution of the level 3 Kodiak DEM.

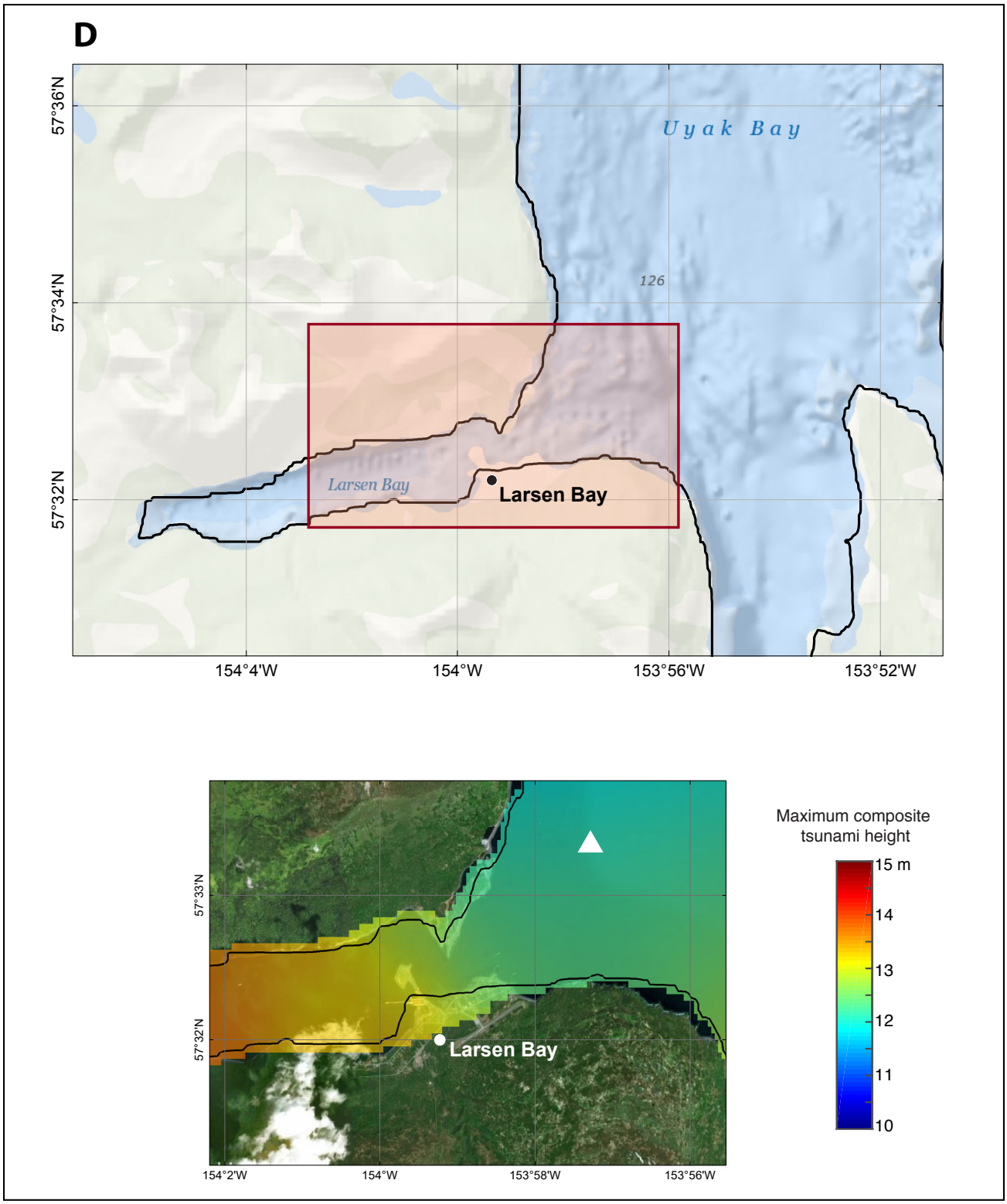

Figure 6D. Maximum composite tsunami height at Larsen Bay. The white triangle indicates the location of the time series point, and the black line is the MHHW shoreline. The pink shaded rectangle in the upper map indicates the area shown in the lower map. The mismatch between the coastlines of the base imagery and the MHHW coastlines is due to low resolution of the level 3 Kodiak DEM.

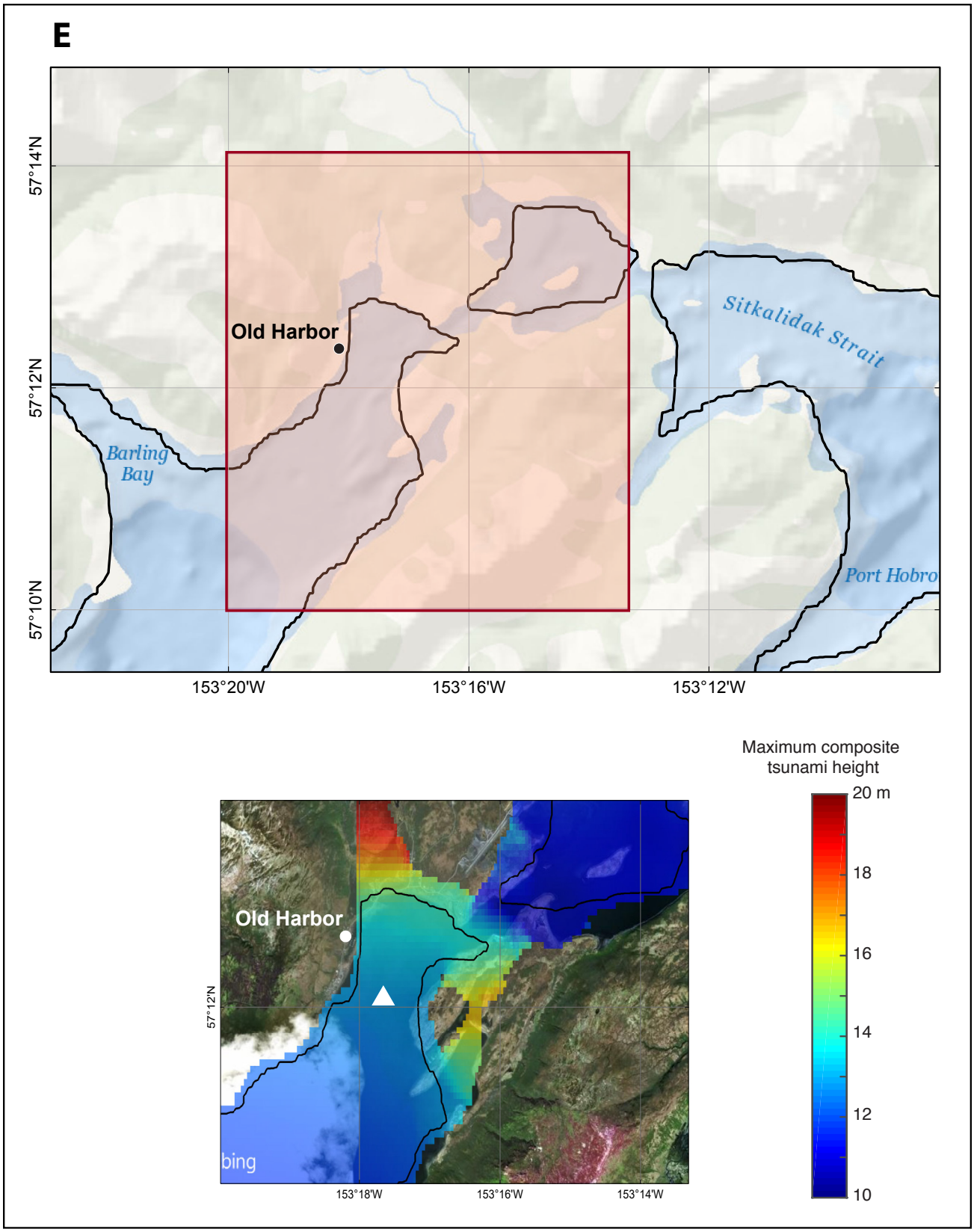

Figure 6E. Maximum composite tsunami height at Old Harbor. The white triangle indicates the location of the time series point, and the black line is the MHHW shoreline. The pink shaded rectangle in the upper map indicates the area shown in the lower map. The mismatch between the coastlines of the base imagery and the MHHW coastlines is due to low resolution of the level 3 Kodiak DEM.

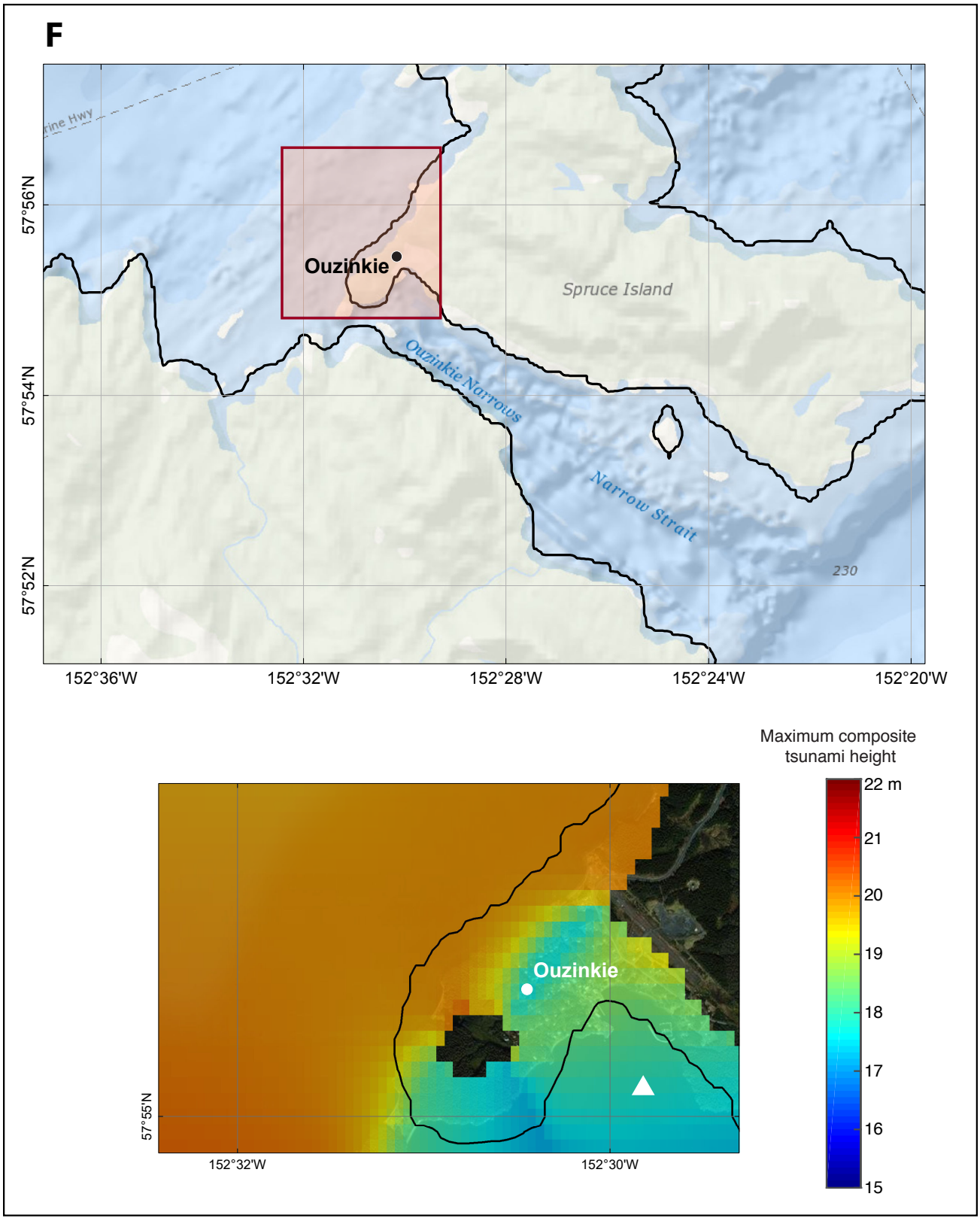

Figure 6F. Maximum composite tsunami height at Ouzinkie. The white triangle indicates the location of the time series point, and the black line is the MHHW shoreline. The pink shaded rectangle in the upper map indicates the area shown in the lower map. The mismatch between the coastlines of the base imagery and the MHHW coastlines is due to low resolution of the level 3 Kodiak DEM.

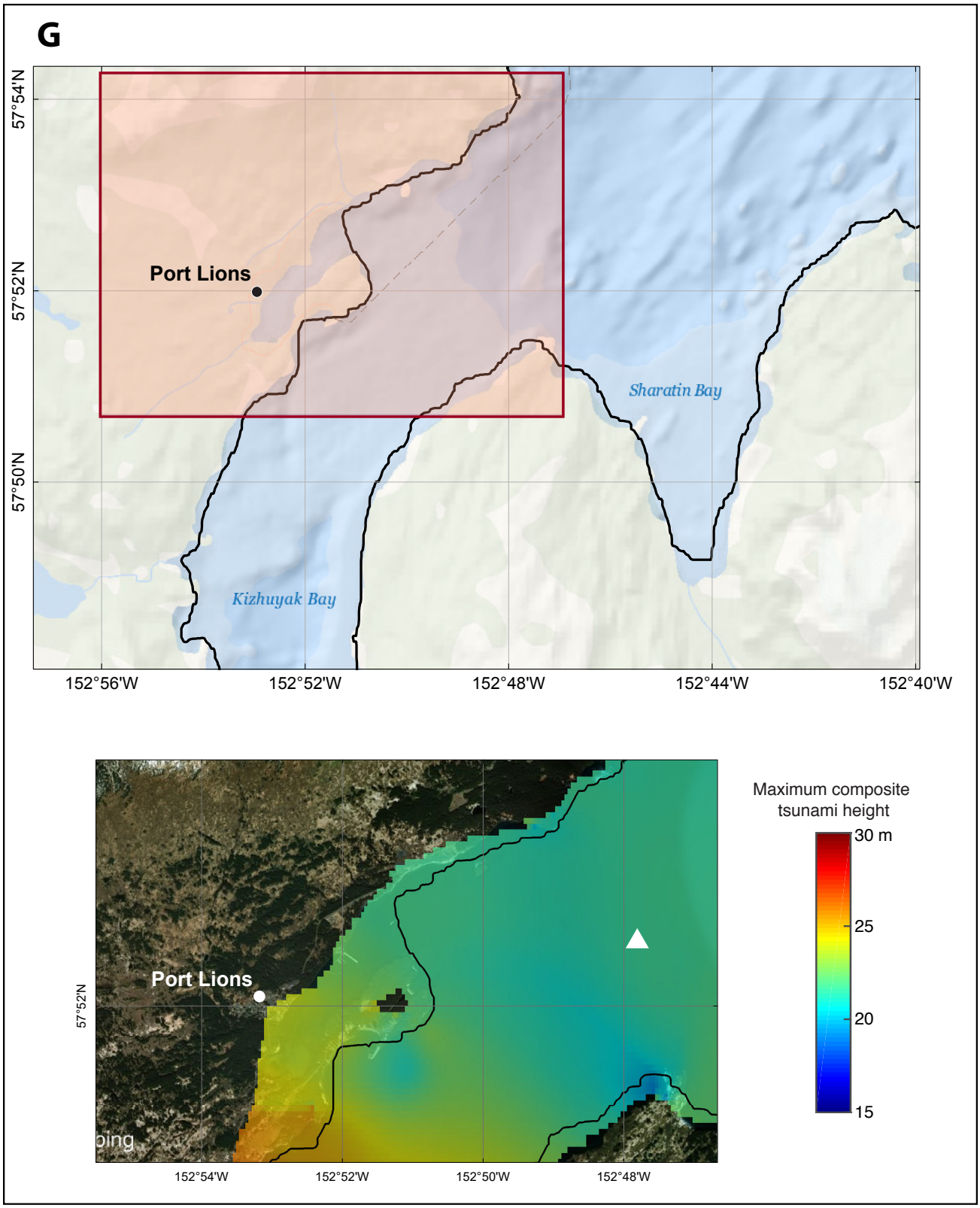

Figure 6G. Maximum composite tsunami height at Port Lions. The white triangle indicates the location of the time series point, and the black line is the MHHW shoreline. The pink shaded rectangle in the upper map indicates the area shown in the lower map. The mismatch between the coastlines of the base imagery and the MHHW coastlines is due to low resolution of the level 3 Kodiak DEM.

plots demonstrate that dangerous waves may arrive as many as 6 hours after the earthquake. Tsunami wave heights in the time series differ from the maximum composite tsunami heights presented in table 4 for each community because the time series show the water level fluctuations at specific points offshore, which are not necessarily the locations where the highest waves occur.

In addition to the time series of the simulated water level, we have also modeled the potential permanent subsidence in the communities. The yellow lines in map sheets 1–7 show the post-earthquake MHHW shoreline after ground subsidence. Scenario 2 results in the largest amounts of subsidence in Chiniak, Larsen Bay, Ouzinkie, and Port Lions (table 3). Most low-lying areas in all communities could be permanently flooded as a result of the earthquakes considered in this report.

SUMMARY

We present the results of modeling earthquake-generated tsunamis in the region of Kodiak Island, and their effects on the Kodiak communities of Akhiok, Chiniak, Karluk, Larsen Bay, Old Harbor, Ouzinkie, and Port Lions. We numerically model tsunami waves generated by local hypothetical tectonic sources, analyze tsunami wave dynamics in the vicinity of the communities, and develop tsunami hazard maps. We compute the composite maximum wave height from nine considered scenarios and follow NTHMP guidelines to extrapolate the modeling data on land for estimation of tsunami inundation. The maximum runup heights are 14 m (46 ft) in Akhiok, 31 m (102 ft) in Chiniak, 11 m (36 ft) in Karluk, 18 m (59 ft) in Larsen Bay, 27 m (89 ft) in Old Harbor, 26 m (85 ft) in Ouzinkie, and 34 m (112 ft) in Port Lions.

Tsunami inundation approximations shown on the tsunami hazard maps have been completed using the best information available and are believed to be accurate; however, their preparation required many assumptions. In this assessment, we estimate the potential tsunami inundation zone based on nine significant characteristic tsunami scenarios. Hence, the modeled tsunami inundation cannot be considered exhaustive, but the modeling results are still thought to provide a sound approximation to the potential tsunami inundation zone in each community.

Actual conditions during a tsunami may differ from the scenarios considered here due to variations in the source earthquakes, tides, and coastline infrastructure. These areas of maximum expected inundation are intended to assist in planning tsunami evacuation and response activities. Results are not suitable for land-use regulation or building-code development.

ACKNOWLEDGMENTS

This project received support from the National Oceanic and Atmospheric Administration (NOAA) under Reimbursable Services Agreement ADN 952011 with the State of Alaska's Division of Homeland Security & Emergency Management (a division of the Department of Military and Veterans Affairs). Numerical calculations for this work were supported by a grant of High Performance Computing (HPC) resources from the Arctic Region Supercomputing Center (ARSC) at the University of Alaska Fairbanks. We thank Jeff Freymueller for his review that helped to improve the report. We are grateful to Rob Witter and Peter Haeussler for their review of potential tsunami sources.

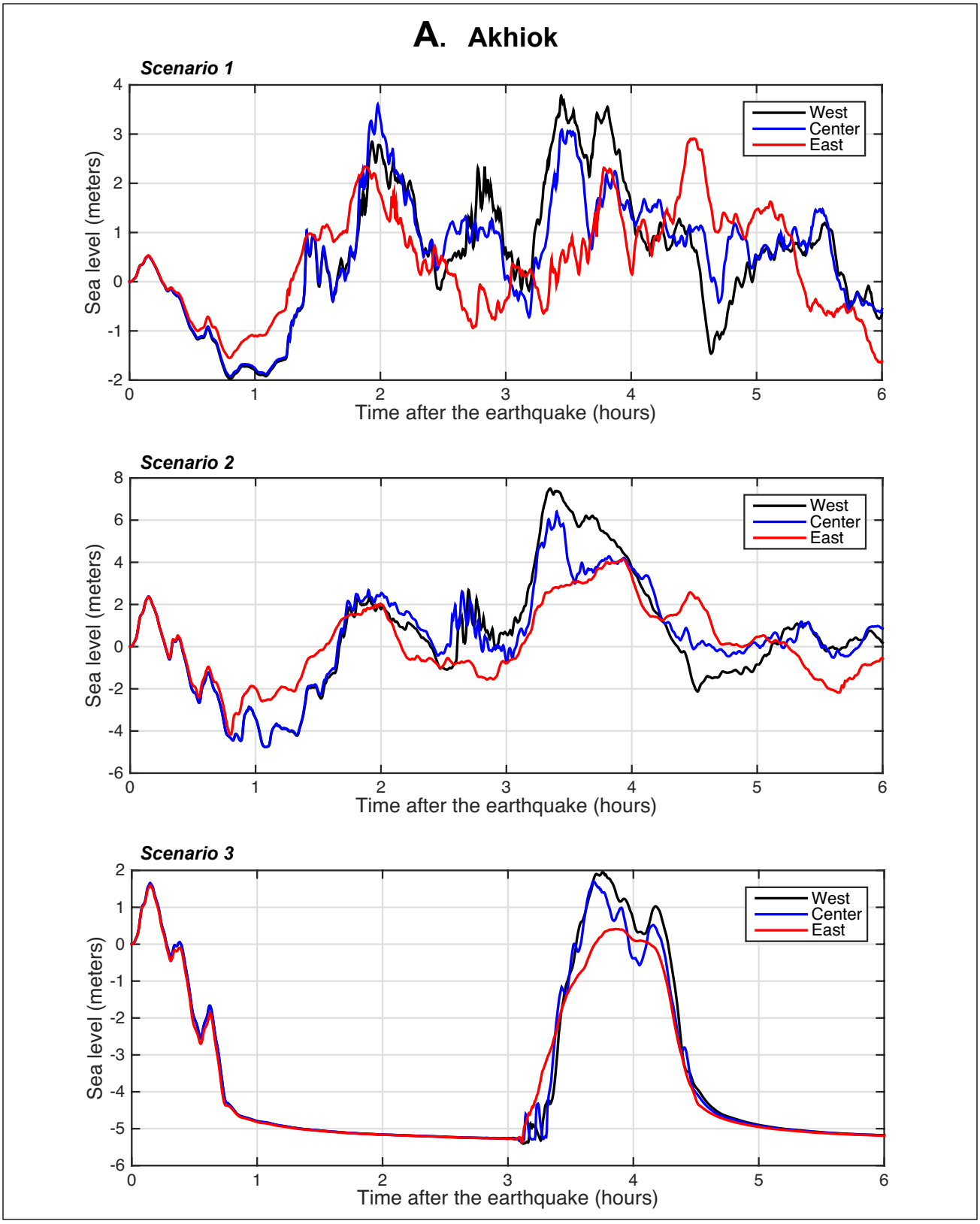

Figure 7A. Time series of water level for scenarios 1–3 at Akhiok, calculated at the locations marked by white triangle in figure 6A.

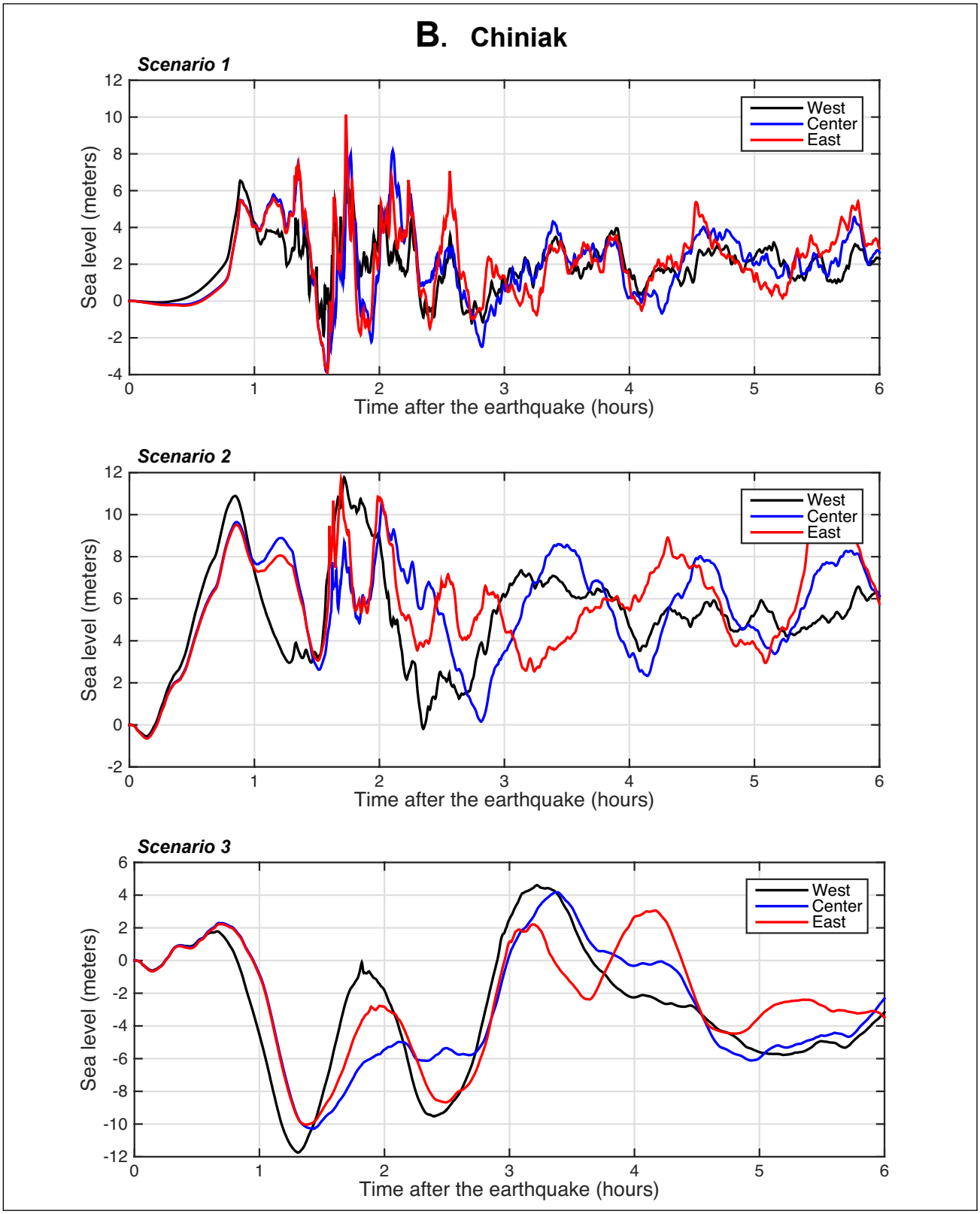

Figure 7B. Time series of water level for scenarios 1–3 at Chiniak, calculated at the locations marked by white triangle in figure 6B.

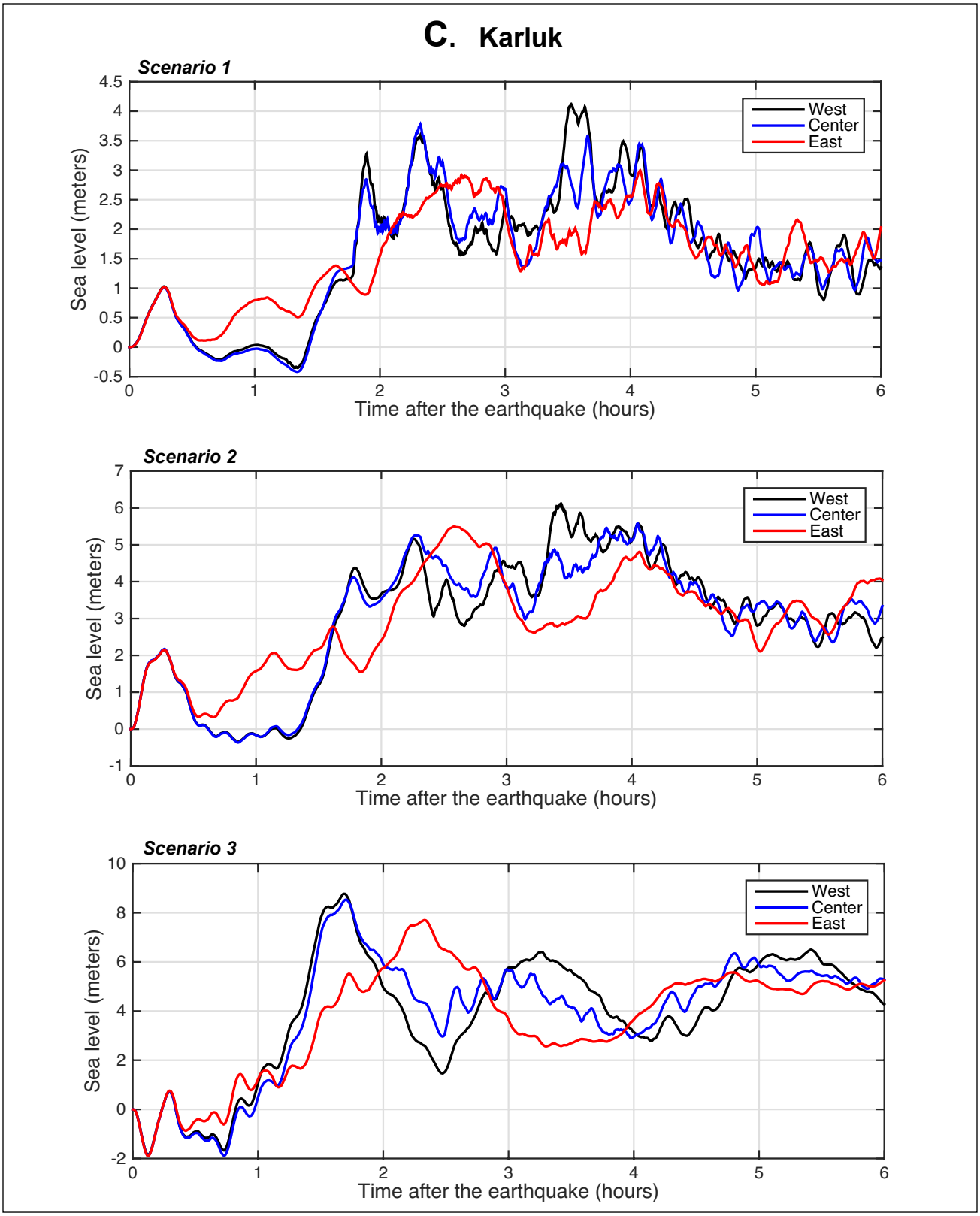

Figure 7C. Time series of water level for scenarios 1–3 at Karluk, calculated at the locations marked by white triangle in figure 6C.

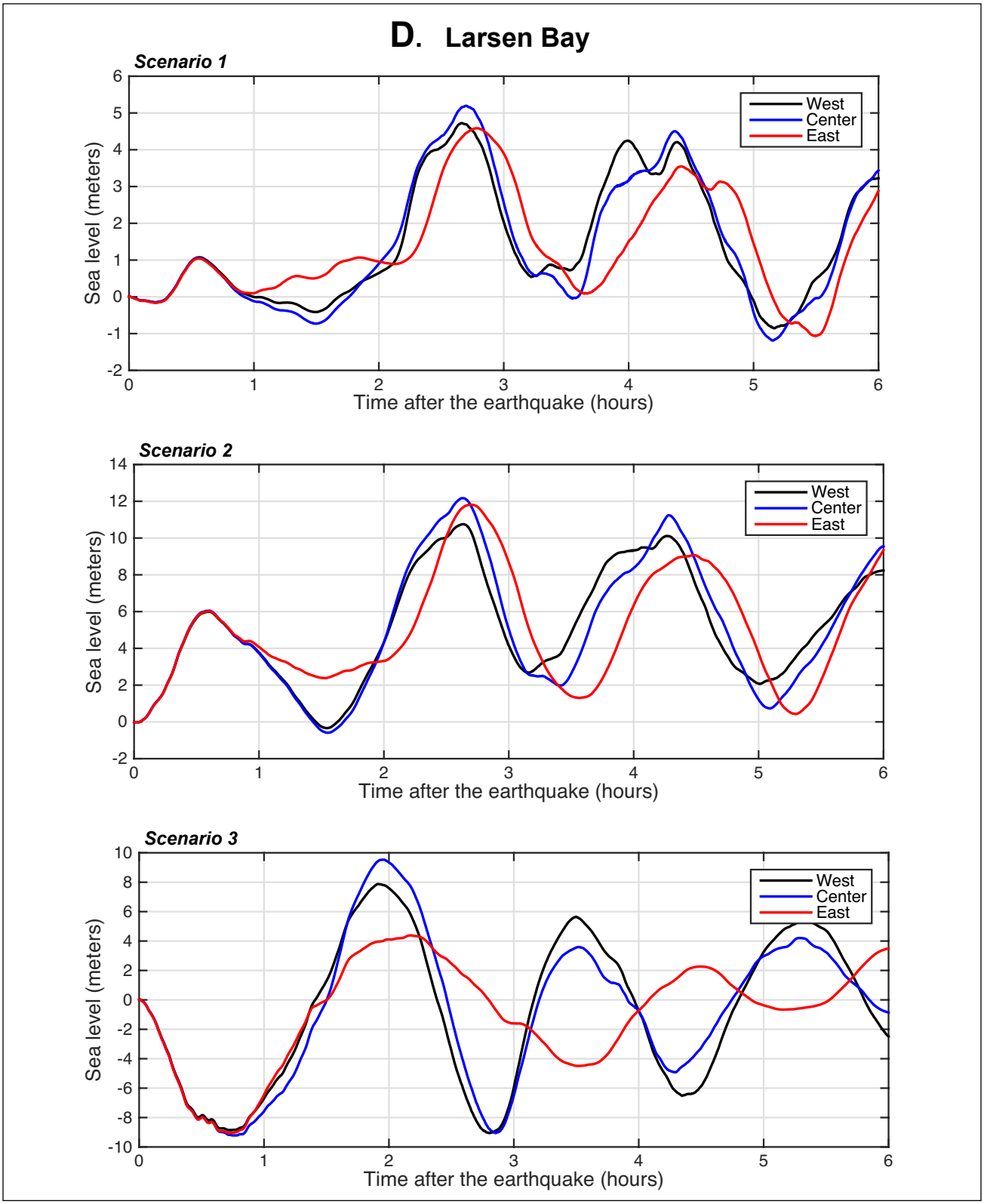

Figure 7D. Time series of water level for scenarios 1–3 at Larsen Bay, calculated at the locations marked by white triangle in figure 6D.

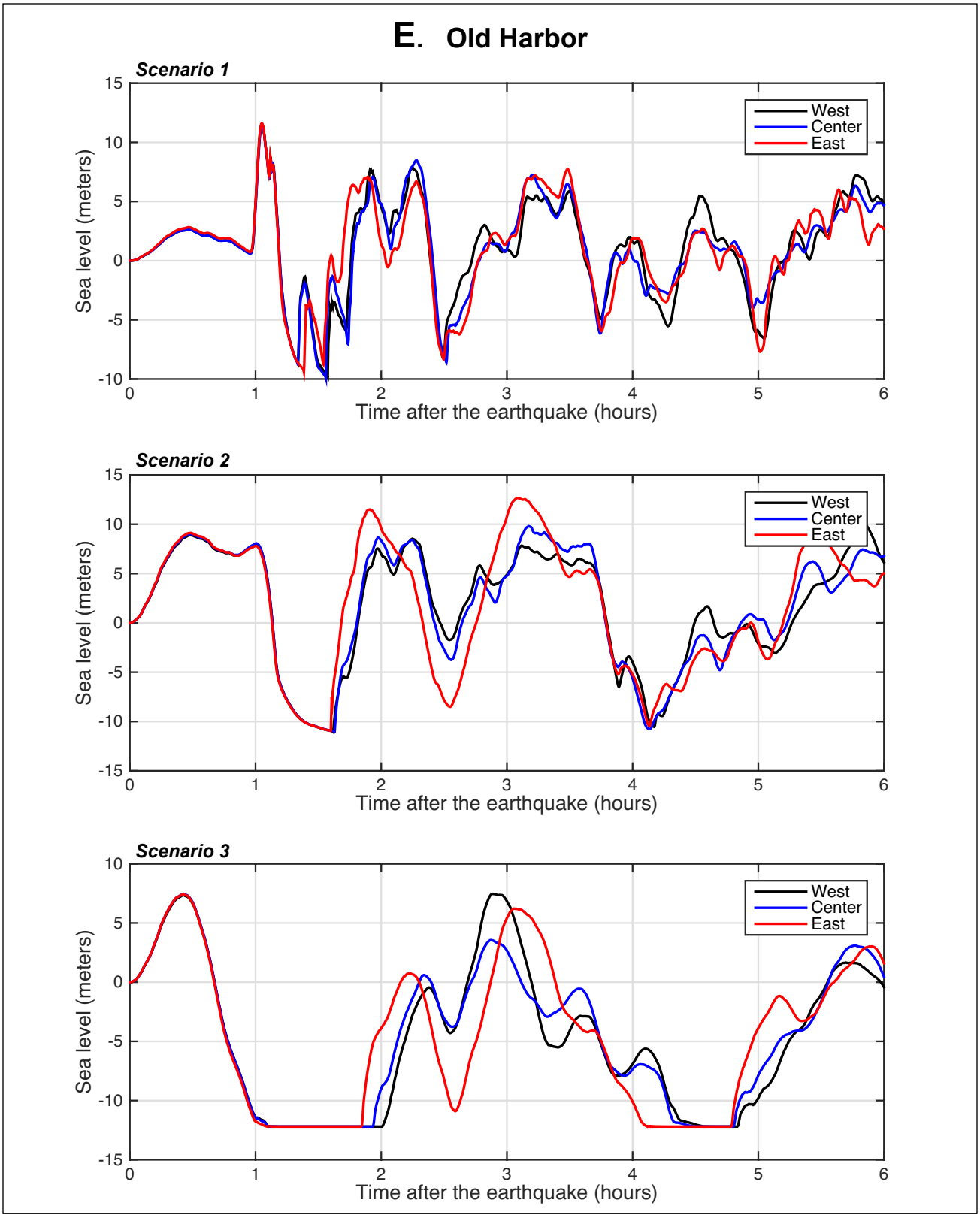

Figure 7E. Time series of water level for scenarios 1–3 at Old Harbor, calculated at the locations marked by white triangle in figure 6E.

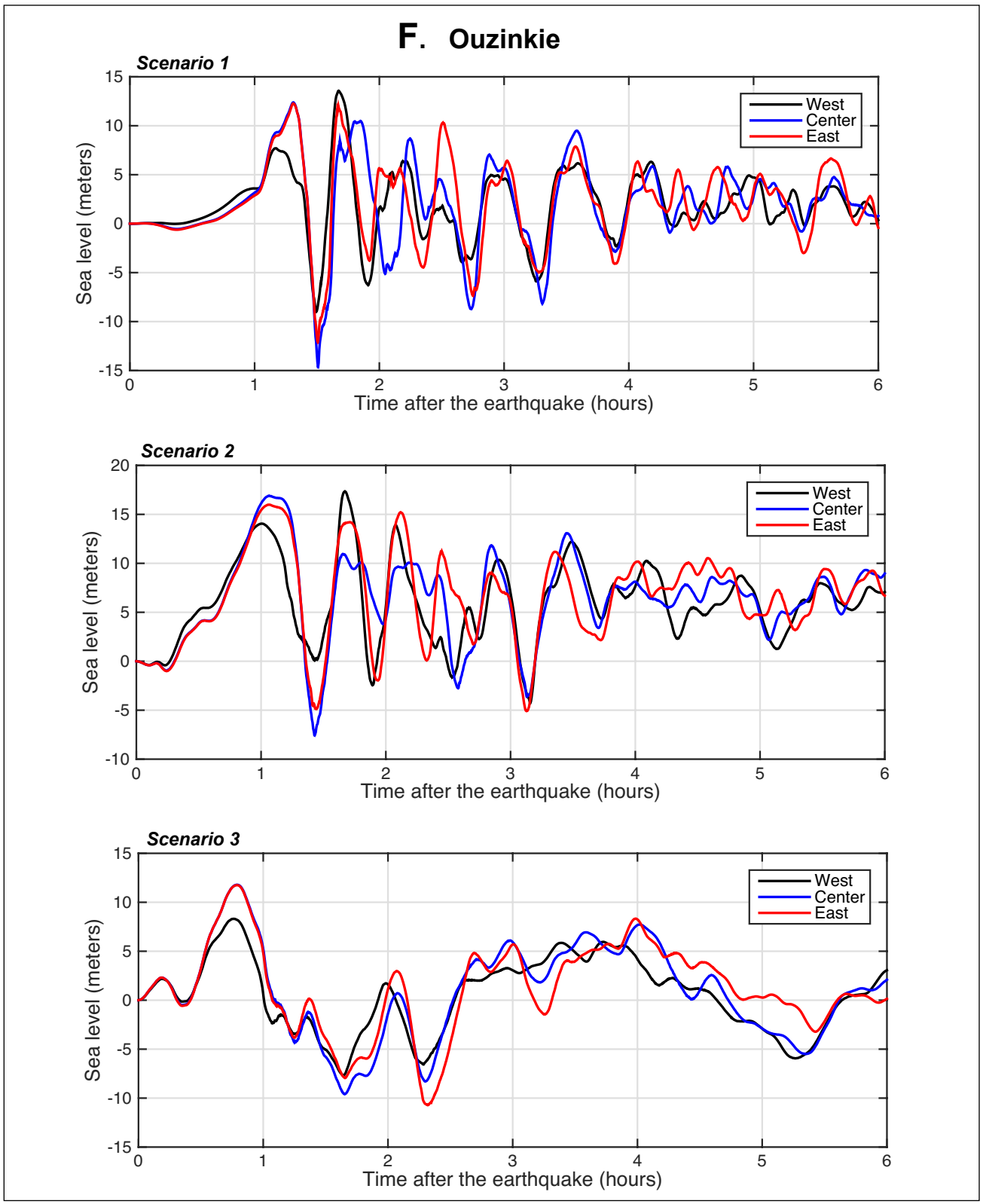

Figure 7F. Time series of water level for scenarios 1–3 at Ouzinkie, calculated at the locations marked by white triangle in figure 6F.

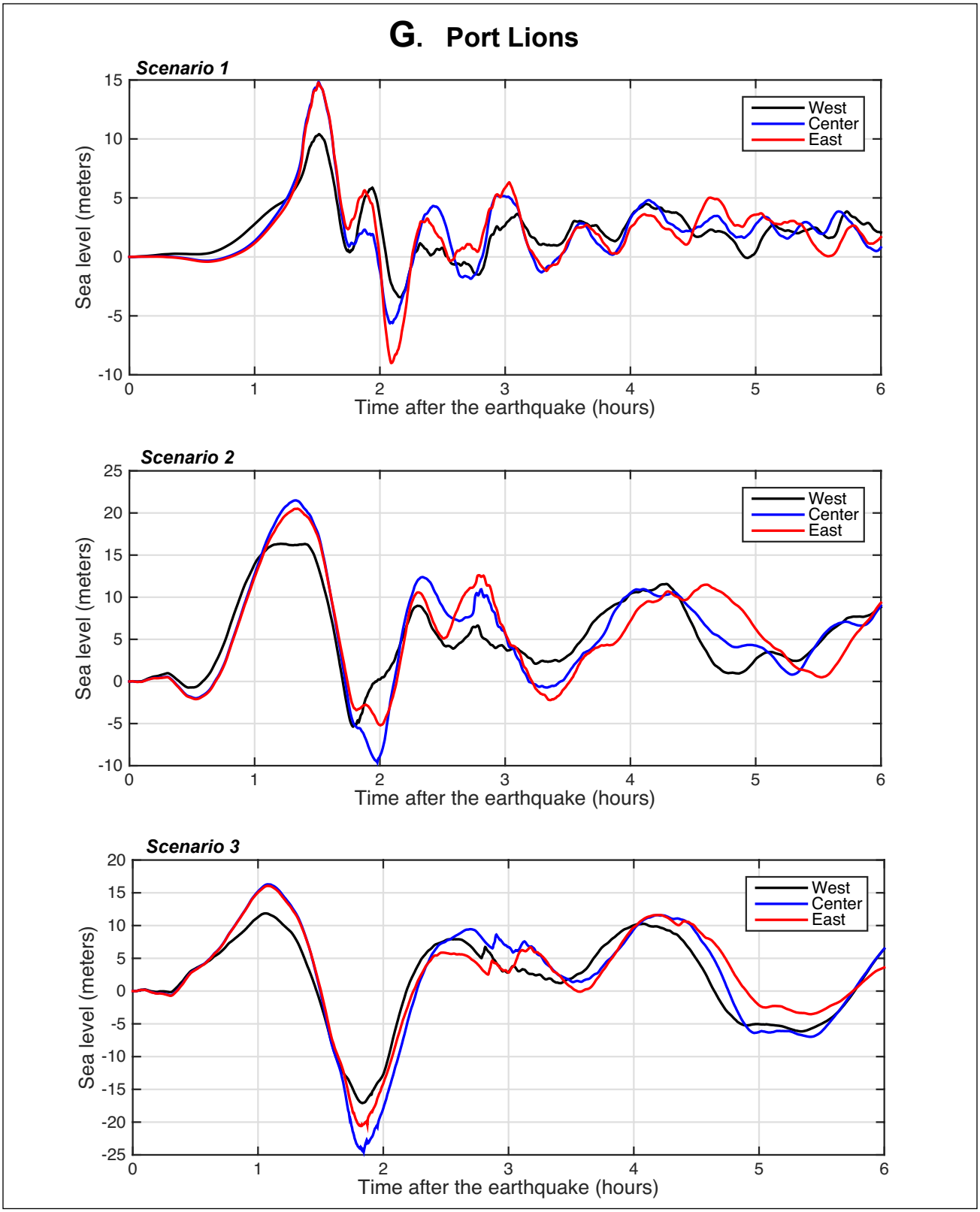

Figure 7G. Time series of water level for scenarios 1–3 at Port Lions, calculated at the locations marked by white triangle in figure 6G.

REFERENCES

Alaska Department of Commerce, Community and Economic Development, Division of Community and Regional Affairs (DCCED/DCRA), 2013. dcra-cdo-dcced.opendata.arcgis.com/

Briggs, R.W., Engelhart, S.E., Nelson, A.R., Dura, T., Kemp, A.C., Haeussler, P.J., Corbett, D.R., Angster, S.J., and Bradley, L.-A., 2014, Uplift and subsidence reveal a nonpersistent megathrust rupture boundary (Sitkinak Island, Alaska): Geophysical Research Letters, v. 41, no. 7, p. 2,289–2,296. doi.org/10.1002/2014GL059380

DeMets, Charles. Gordon, R.C., Argus, D.F., and Stein, Seth, 1990, Current plate motions: Geophysical Journal International, v. 101, no. 2, p. 425–478.

Estabrook, C.H., Jacob, K.H., and Sykes, L.R., 1994, Body wave and surface wave analysis of large and great earthquakes along the eastern Aleutian arc, 1923–1993; Implications for future events: Journal of Geophysical Research, v. 99, no. B6, p. 11,643–11,662.

Fujii, Yushiro, Satake, Kenji, Sakai, Shin'ichi, Shinohara, Masanao, and Kanazawa, Toshihiko, 2011, Tsunami source of the 2011 off the Pacific coast of Tohoku earthquake: Earth Planets Space, v. 63, p. 815–820. terrapub.co.jp/journals/EPS/pdf/2011/6307/63070815.pdf

Geist, L.G., and Parsons, T., 2006, Probabilistic analysis of tsunami hazards: Natural Hazards, v. 37, no. 3, p. 277–314. doi.org/10.1007/s11069-005-4646-z

Johnson, J.M., Tanioka, Yuichiro, Ruff, L.J., Satake, Kenji, Kanamori, Hiroo, and Sykes, L.R., 1994, The 1957 great Aleutian earthquake, Pure and Applied Geophysics, v. 142, no. 1, p. 3–28. doi.org/10.1007/BF00875966

Kanamori, Hiroo, 1970, The Alaska earthquake of 1964; Radiation of long-period surface waves and source mechanism: Journal of Geophysical Research, v. 75, no. 26, p. 5,029–5,040.

Kirby, Stephen, Scholl, David, von Huene, Roland, and Wells, Ray, 2013, Alaska earthquake source for the SAFRR tsunami scenario, chapter B, *in* Ross, S.L., and Jones, L.M., eds., The SAFRR (Science Application for Risk Reduction) Tsunami Scenario: U.S. Geological Survey Open-File Report 2013–1170, 40 p. pubs.usgs.gov/of/2013/1170/b/

Lander, J.F., 1996, Tsunamis affecting Alaska, 1737–1996: Boulder, CO, National Oceanic and Atmospheric Administration, National Geophysical Data Center (NGDC), Key to Geophysical Research Documentation, v. 31, 155 p.

Lim, E., Eakins, B.W., and Wigley, R., 2011, Coastal relief model of southern Alaska; Procedures, data sources and analysis: NOAA Technical Memorandum NESDIS NGDC-43, 22 p.

Lopez, A.M., and Okal, E.A., 2006, A seismological reassessment of the source of the 1946 Aleutian 'tsunami' earthquake: Geophysical Journal International, v. 165, no. 3, p. 835–849. doi.org/10.1111/j.1365-246X.2006.02899.x

Macpherson, A.E., Nicolsky, D.J., and Suleimani, E.N., 2014, Digital elevation models of Skagway and Haines, Alaska: Procedures, data sources, and quality assessment: Alaska Division of Geological & Geophysical Surveys Miscellaneous Publication 155, 15 p. doi.org/10.14509/29143

National Geophysical Data Center (NGDC), 2006, 2-minute Gridded Global Relief Data (ETOPO2) v2: National Geophysical Data Center (NGDC), National Oceanic and Atmospheric Administration (NOAA). doi.org/10.7289/V5J1012Q

National Geophysical Data Center/World Data Service (NGDC/WDS), continuously updated, Global historical tsunami database at NGDC, 2100 BC to present (interactive map): National Oceanic and Atmospheric Administration (NOAA), National Geophysical Data Center (NGDC). doi.org/10.7289/V5PN93H7

National Tsunami Hazard Mapping Program (NTHMP), 2010, Guidelines and best practices for tsunami inundation modeling for evacuation planning: National Oceanic and Atmospheric Administration (NOAA), NTHMP Mapping & Modeling Subcommittee.

———2012, Proceedings and results of the 2011 NTHMP Model Benchmarking Workshop: Boulder, CO, U.S. Department of Commerce/NOAA/NTHMP, NOAA Special Report, 436 p. nthmp.tsunami.gov

Nicolsky, D.J., Suleimani, E.N., Combellick, R.A., and Hansen, R.A., 2011a, Tsunami inundation maps of Whittier and western Passage Canal, Alaska: Alaska Division of Geological & Geophysical Surveys Report of Investigation 2011-7, 65 p. doi.org/10.14509/23244

Nicolsky, D.J., Suleimani, E.N., Haeussler, P.J., Ryan, H.F., Koehler, R.D., Combellick, R.A., and Hansen, R.A., 2013, Tsunami inundation maps of Port Valdez, Alaska: Alaska Division of Geological & Geophysical Surveys Report of Investigation 2013-1, 77 p., 1 sheet, scale 1:12,500. doi.org/10.14509/25055

Nicolsky, D.J., Suleimani, E.N., and Hansen, R.A., 2011b, Validation and verification of a numerical model for tsunami propagation and runup: PUre and Applied Geophysics, v. 168, p. 1,199–1,222. doi.org/10.1007/s00024-010-0231-9

Nicolsky, D.J., Suleimani, E.N., and Koehler, R.D., 2014, Tsunami inundation maps of Cordova and Tatitlek, Alaska: Alaska Division of Geological & Geophysical Surveys Report of Investigation 2014-1, 49 p. doi.org/10.14509/27241

Plafker, George, 1969, Tectonics of the March 27, 1964, Alaska earthquake: U.S. Geological Survey Professional Paper 543-I, 74 p.

Ross, S.L., Jones, L.M., Miller, Kevin, P., K.A., Wein, A., Wilson, Ri.I., Bahng, B., Barberopoulou, A., Borrero, J.C., Brosnan, D.M., Bwarie, J.T., Geist, E.L., Johnson, L.A., Kirby, S.H., Knight, W.R., Long, K., Lynett, P., Mortensen, C.E., Nicolsky, D.J., Perry, S.C., Plumlee, G.S., Real, C.R., Ryan, K., Suleimani, E., Thio, H., Titov, V.V., Whitmore, P.M. and Wood, N.J., 2013, SAFRR (Science Application for Risk Reduction) Tsunami Scenario—Chapter A, Executive Summary and Introduction, *in* Ross, S.L., and Jones, L.M., eds., The SAFRR Tsunami Scenario: U.S. Geological Survey Open-File Report 2013–1170, p. 1–17. pubs.usgs.gov/of/2013/1170/

Shao, Guangfu, Li, Xiangyu, Ji, Chen, and Maeda, Takahiro, 2011, Focal mechanism and slip history of 2011 M_W 9.1 off the Pacific coast of Tohoku earthquake, constrained with teleseismic body and surface waves: Earth Planets Space, v. 63, no. 7, p. 559–564. doi.org/10.5047/eps.2011.06.028

Suleimani, E.N., Nicolsky, D.J., and Koehler, R.D., 2013, Tsunami inundation maps of Sitka, Alaska: Alaska Division of Geological & Geophysical Surveys Report of Investigation 2013-3, 76 p., 1 sheet, scale 1:250,000. doi.org/10.14509/26671

Suleimani, E.N., Nicolsky, D.J., and Koehler, R.D., 2015, Tsunami inundation maps of Elfin Cove, Gustavus and Hoonah, Alaska: Alaska Division of Geological & Geophysical Surveys Report of Investigation 2015-1, 79 p. doi.org/10.14509/29404

Suleimani, E.N., Nicolsky, D.J., Koehler, R.D., and Salisbury, J.B., 2018, Regional tsunami hazard assessment for Andreanof Islands, Alaska: Alaska Division of Geological & Geophysical Surveys Report of Investigation 2017-2, 19 p., 2 sheets. doi.org/10.14509/29704

Suleimani, E.N., Nicolsky, D.J., West, D.A., Combellick, R.A., and Hansen, R.A., 2010, Tsunami inundation maps of Seward and Northern Resurrection Bay, Alaska: Alaska Division of Geological & Geophysical Surveys Report of Investigation 2010-1, 47 p., 3 sheets, scale 1:12,500. doi.org/10.14509/21001

Synolakis, C.E., Bernard, E.N., Titov, V.V., Kânoğlu, U., and González, F.I., 2007, Standards, criteria, and procedures for NOAA evaluation of tsunami numerical models: Seattle, WA, NOAA/Pacific Marine Environmental Laboratory, Technical Memorandum OAR PMEL-135, 55 p.

Wu, F.T., and Kanamori, Hiroo, 1973, Source mechanism of February 4, 1965, Rat Island earthquake: Journal of Geophysical Research, v. 78, no. 26, p. 6,082–6,092.